SIMULATING AND OPTIMIZING A ZERO-WASTE WAVE-TO-WATER DESALINATION SYSTEM

by

Gabriel Glosson

May, 2023

Director of Thesis: Faete Filho, Ph.D.
Major Department: Mechanical Engineering

Abstract

Current methods of producing clean water are not capable of meeting growing demands. One method of producing clean water is through a process called desalination, which is the process of removing salt and other minerals from seawater. However, traditional desalination methods can be energy-intensive and generate significant amounts of waste. To help address these issues, a hybrid wave-to-water desalination system that combines reverse osmosis (RO) with supercritical water desalination (SCWD) can produce freshwater from seawater. SCWD treats the brine produced by RO, while RO produces freshwater at a lower energy cost. The system utilizes an oscillating surge wave energy converter (OSWEC) to harness the energy of ocean waves to directly pressurize the seawater feeding into the RO system. Using ocean waves as an energy source makes the system renewable and reduces the carbon footprint of the desalination process. This thesis presents the development of a simulation for a small-scale zero-waste desalination system powered by off-grid renewable energy. The model of the system was developed using MATLAB Simulink along with WEC-Sim. A sensitivity analysis was performed on the model to determine the optimal configuration of key system parameters. The sensitivity analysis was conducted using an irregular wave pattern with a significant wave height of 0.117 m and a period of 1.68 s. The parameters investigated in the sensitivity analysis were the system's power take-off (PTO) volumetric displacement,

accumulator size, and RO membrane type. The results of the sensitivity analysis showed that the optimized system was the one that used an SW30HR-380 RO membrane, a PTO volumetric displacement of 1975 cm^3/rad, and a 10-gallon accumulator. The average water production rate for the optimized system was 32.644 gpm.

Simulating and Optimizing a Zero-Waste Wave-To-Water Desalination System

A Thesis

Presented to the Faculty of the Department of Engineering

East Carolina University®

In Partial Fulfillment of the Requirements for the Degree

Masters of Science in Mechanical Engineering

by

Gabriel Glosson

May, 2023

©2023, Gabriel Glosson

Simulating and Optimizing a Zero-Waste Wave-To-Water Desalination System

by

Gabriel Glosson

APPROVED BY:

Director of Thesis

Faete Filho, Ph.D.

Committee Member

Tarek Abdel-Salam, Ph.D.

Committee Member

Kurabachew Duba, Ph.D.

Committee Member

Jinbo Chen, Ph.D.

Chair of the Department of Engineering

Barbara Muller-Borer, Ph.D.

Dean of the Graduate School

Kathleen Cox, Ph.D.

Acknowledgements

I want to express my gratitude to several people who have supported me throughout my research and academic journey. First and foremost, I would like to thank my advisor, Dr. Faete Filho, for his guidance, encouragement, and unwavering support throughout my undergraduate and graduate studies. His expertise and feedback were instrumental in the completion of this thesis.

I would also like to thank Dr. Jinbo Chen for his assistance with the supercritical water desalination system. I want to thank my entire committee, Dr. Tarek Abdel-Salam, Dr. Kurabachew Duba, and Dr. Jinbo Chen, for their time and feedback.

I want to thank my professors for their guidance and advice during my time in the program. I also want to thank my fellow students for their help and support. In particular, I would like to thank Jason McMorris for his assistance with the hydrodynamics for the wave energy converter.

Finally, I want to thank my family and friends for their constant support, encouragement, and understanding throughout my academic journey.

Contents

List of Tables

List of Figures

List of Acronyms

BEMIO	Boundary Element Method Input/Output
ED	Electrodialysis
MED	Multi-Effect Distillation
MSF	Multi-Stage Flash
NF	Nanofiltration
OSWEC	Oscillating Surge Wave Energy Converter
PTO	Power Take-Off
REFPROP	Reference Fluid Thermodynamic and Transport Properties Database
RO	Reverse Osmosis
SCWD	Supercritical Water Desalination
WAVE	Water Application Value Engine
WEC	Wave Energy Converter
WEC-Sim	Wave Energy Converter Simulator
ZLD	Zero Liquid Discharge

Nomenclature

$\%R$	Target recovery ratio or percent recovery
$\Delta\pi$	Osmotic pressure
Δp	Reverse osmosis feed pressure
ρ	Fluid density
A_ω	Permeability coefficient
A_m	Active membrane surface area
A_{FR}	Flow restrictor area
B_s	Solute transport parameter
B_{lam}	Pressure ratio at the laminar and turbulent regime transition point
C_m	Reverse osmosis feed solute concentration
C_p	Permeate solute concentration
$P_{a,FR}$	Flow restrictor inlet pressure
P_{atm}	Atmospheric pressure
$P_{avg,FR}$	Average pressure across the flow restrictor

$P_{b,FR}$ Flow restrictor outlet pressure

P_{cr} Minimum pressure for turbulent flow during the transition from laminar to the turbulent regime

Q_F Reverse osmosis feed flow rate

Q_p Permeate flow rate

Q_{Target} Flow restrictor target flow rate

R Membrane resistance

Chapter 1

Introduction

The global demand for water is steadily increasing, particularly in areas with limited water resources. It is estimated that approximately four billion people globally live in severe water-scarce areas for at least one month of the year, with half a billion people living in water-scarce regions year-round[1]. Furthermore, twenty-five percent of the world's large cities face water stress from not meeting the demand for clean water[2]. Current methods of producing clean water are not able to meet demands. Over 97% of the earth's water is in the ocean but contains too much salt for human consumption[3]. One possible method of utilizing this large amount of water is through desalination, which is a process that removes salt and mineral content from seawater to make it consumable for humans.

The most commonly used type of desalination is Reverse Osmosis (RO), with approximately 84% of all desalination systems using RO and 69% of all desalinated water coming from it[4]. RO uses a semi-permeable membrane to separate pressurized seawater into fresh water and brine. Brine is a water solution with a large salt concentration, which is toxic to the environment if not properly disposed of. Some of the most commonly used methods for brine disposal include discharging the brine directly into the ocean, deep-well injection, surface water discharge, sewer discharge, and brine evaporation ponds[4,5]. Each of these

brine disposal methods has a negative impact on the environment. One of the reasons RO is the leading method for desalination is that it is one of the most energy-efficient forms of desalination.

Another type of desalination is Supercritical Water Desalination (SCWD). In SCWD, the temperature and pressure of seawater are raised until the water reaches a supercritical state, which is approximately a temperature greater than 374°C and a pressure greater than 221 bar. The properties of water change significantly at this point, making it significantly easier to separate the salt from the water fully. This type of desalination system is known as a Zero Liquid Discharge (ZLD) system, meaning it does not produce brine. The main issue with SCWD is the larger energy requirement compared to other desalination techniques. The desalination system used in this research is a hybrid desalination system that utilizes both RO and SCWD. The SCWD system eliminates the brine produced by the RO membrane, while the RO membrane reduces the system's energy requirements.

One of the main issues with desalination technologies is that desalination is an energy-intensive process. It is estimated that 45 to 65 million dollars a year is spent on energy for desalination in the United States alone[6]. This high energy demand currently results in higher use of fossil fuels and greenhouse gas emissions. Renewable energy systems have lower operational costs than nonrenewable options, and renewable energy produces less greenhouse gas emissions[7]. Wave energy has a high potential for use in a desalination system because it is a reliable energy source and has high energy potential[8]. One way of harvesting wave energy is by using a device called a Wave Energy Converter (WEC). An Oscillating Surge Wave Energy Converter (OSWEC) is a type of WEC that has a fixed base and a hinged flap that oscillates from the waves colliding with it. One advantage of using an OSWEC for desalination is that it can directly pressurize and pump water into the desalination system. Directly pressurizing water results in fewer energy losses because there are no losses from converting between mechanical and electrical energy. Additionally, if the desalination system

is powered by off-grid renewable energy instead of being attached to a grid, then the system can be used in more remote locations.

This thesis discusses the development and optimization of a simulation of a 1:15 scale hybrid desalination system that was powered by an OSWEC and utilized both SCWD and RO desalination. The model of the system was developed in MATLAB Simulink. The model of the WEC was developed using Wave Energy Converter Simulator (WEC-Sim), which is an open-source MATLAB-based simulation tool developed by the National Renewable Energy Laboratory (NREL) and Sandia National Laboratories (Sandia)[9]. The geometry of the WEC was modeled in SolidWorks, and the hydrodynamics of the flap were simulated using WAMIT, which is a wave analysis tool developed by the Massachusetts Institute of Technology. The hydrodynamic data from WAMIT was used as an input into the WEC-Sim model. The Power Take-Off (PTO) was modeled using MATLAB Simscape. Water Application Value Engine (WAVE) is a program that is frequently used to simulate and design membrane-based desalination systems. The model of the RO membrane was developed in Simulink using information obtained from a model of the membrane developed in WAVE. The SCWD system was modeled in Simulink and used a series of equations to determine basic thermodynamic properties, energy consumption, and other essential system parameters for each component of the SCWD system.

A sensitivity analysis was performed on the numerical model of the complete system to optimize the system. In the sensitivity analysis, three key parameters of the system were investigated: the volumetric displacement of the PTO, the accumulator size, and the type of RO membrane. The sensitivity analysis was performed using the multiple condition run (MCR) function provided by WEC-Sim, and a custom MATLAB application was developed for analyzing the results from the sensitivity analysis.

Section 2 contains background information used in this research. Section 2.1 covers desalination, reverse osmosis, supercritical water desalination, and current brine disposal

methods and their associated environmental impact. Section 2.2 covers wave energy converters, with a focus on oscillating surge wave energy converters. Section 2.3 covers current research on wave-powered desalination. Discussed in Section 3 is the methodology used for developing the numerical model of the system and the sensitivity analysis performed on the system. Section 4 contains the results and discussion of the sensitivity analysis, and Section 6 summarizes and concludes the research covered in this thesis.

Chapter 2

Background

2.1 Desalination

Desalination is the process of removing salt and other minerals from seawater in order to make it safe for human consumption or irrigation. This process is commonly used in areas where freshwater resources are scarce, and it has become an increasingly important source of water in arid and semi-arid regions. Desalination can be achieved through a variety of different methods, which can be broadly classified into two main categories: membrane-based and thermal-based desalination.

Membrane-based desalination is a method that utilizes semi-permeable membranes to separate the salt and other minerals from seawater. The most widely used type of membrane-based desalination is RO, which is discussed further in Section 2.1.1. Another type of membrane desalination is Nanofiltration (NF). Like RO, NF uses a pressure gradient across a membrane. NF membranes have larger pores than RO membranes, so they are not typically used for seawater desalination. Electrodialysis (ED) desalination uses voltage to separate the salt ions and pull them through an anion-permeable membrane. ED is not customarily used for seawater desalination because it has a lower efficiency than other methods, and it

cannot filter out bacteria, and some other substances[10].

Thermal-based desalination, also known as distillation, is a method that utilizes heat to create steam, which is then condensed to create fresh water[11]. The remaining salt and minerals are left behind in the original seawater. The most commonly used methods for thermal-based desalination are Multi-Stage Flash (MSF) and Multi-Effect Distillation (MED), with approximately 2.2% of all desalination systems using MSF, and 5.6% using MED[4,12]. In an MSF system, water flows through pipes and is heated by steam surrounding the pipes as it passes through multiple flash evaporators. After the flash evaporators evaporate the water, it condenses against the feed flow pipe, and a heat exchanger typically recovers some of the heat. This form of desalination can produce very clean water, but it requires tremendous energy[13]. MED works like MSF, but MED has steam flowing through the pipes while the feedwater is poured over the pipe, which causes it to become vapor. MED reuses the heat of the vapor after the first stage, which reduces the amount of energy required by this process compared to MSF[13]. Thermal-based desalination is a more traditional method for desalination. However, there has been a shift to membrane-based desalination due to the higher efficiencies and recovery ratios of membrane-based systems. Traditional thermal-based systems also have a stronger environmental impact from the higher brine production rates and energy consumption. Current systems that use thermal-based desalination are primarily used for water with a high salinity[4].

2.1.1 Reverse Osmosis Desalination

RO is a type of membrane-based desalination, and it is the most used type of desalination, with 84% of all desalination plants using it[4]. The RO process works by applying high pressure to force water through a semi-permeable membrane, leaving the salt and other minerals behind. The permeated water is collected on the other side of the membrane while the brine is discharged. One of the main advantages of RO desalination is that it is one

of the most efficient forms of desalination and requires less energy than most desalination methods. However, it still requires a significant amount of energy to operate, and the cost of electricity is a significant part of the overall cost of the process. Additionally, the RO process generates a large amount of brine, which can have negative environmental impacts if not properly treated or disposed of. Overall, reverse osmosis desalination is a highly effective method for producing fresh water from seawater. However, it does require significant energy, and careful management of the produced brine is important to minimize the environmental impact.

2.1.2 Supercritical Water Desalination

SCWD is an innovative and promising method for desalination that utilizes high-pressure, high-temperature water to remove salt and other dissolved solids from seawater. The process occurs at temperatures and pressures above the critical point of water, which is approximately 374 °C and 221 bar. At these conditions, water exhibits both liquid and gas-like properties, and dissolved salts and other solids can be easily separated from the water[14]. SCWD has several advantages. It can produce water that is a very high quality. SCWD can also desalinate water with much higher salinity than most other forms of desalination. Additionally, SCWD is a process that does not produce any brine, making it a ZLD system. One of the main challenges facing SCWD is the significant energy requirement for operating the system. Additionally, the high-pressure, high-temperature equipment required to operate the process can be expensive and difficult to maintain. Further research and development are needed to improve efficiency and reduce the cost of the process.

A study was done on designing a pilot plant for SCWD with ZLD, which means brine is not a by-product of this desalination method. The proposed design used a high-pressure pump to pressurize the feed flow. The pressurized water then went through a heat exchanger followed by a heater that significantly increased the temperature. With both the pressure

and temperature raised, the water is at the supercritical point. A separator and crystallizer then extract the salt from the water. The water goes through the heat exchanger to recover the heat from the water. The system's outputs are solid salt and drinkable water, but it requires an extremely large amount of energy to operate. Figure 2.1 shows a basic schematic of the system[15].

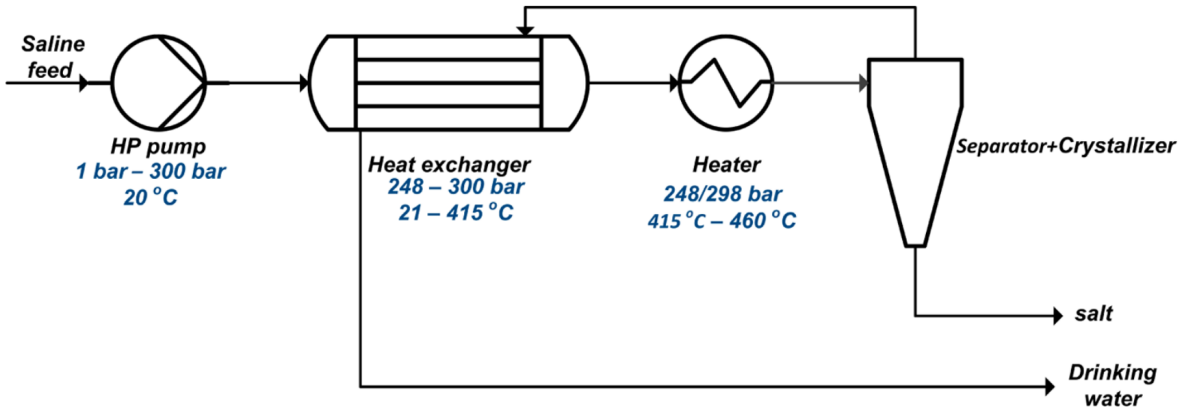

Figure 2.1: Supercritical Water Desalination System[15].

An experimental apparatus was created for this SCWD system to test the system under multiple temperatures and pressures. The experimental setup was used to examine the phases of the water and salt under supercritical conditions through visual inspection using a camera. Past studies investigated the solubility and equilibrium phase diagrams for salt, but it was reasoned that there were large discrepancies in the results of the past studies. As a result, the solubility measurements at phase equilibrium were taken at multiple points of the SCWD experimental system to obtain the salt concentration in the different phases observed by visual inspection. This study also created a simulation for a SCWD system using UniSim Design Suite. The simulation analyzed how various temperatures and pressures affect the heat exchanger and heater. The developed simulation worked under the assumption that the fluid was pure water and neglected the presence of salt in the water. This assumption affected the resulting information with a significant impact on the results for the heat exchanger

performance and the required process energy[15].

2.1.3 Hybrid Desalination System

Hybrid desalination refers to the integration of two or more desalination technologies to produce high-quality potable water while addressing the limitations of individual technologies. A hybrid system can combine thermal, membrane-based, and other desalination methods to achieve improved performance, such as reduced energy consumption, lower brine production, and higher product water quality. The implementation of hybrid desalination is becoming increasingly popular as it has been shown to provide a more sustainable and cost-effective approach to producing potable water from various water sources. It is important to note that while hybrid desalination systems can offer many benefits, they also require more complex design and operation, as well as higher maintenance costs compared to single-stage systems.

A recent study was done to develop a hybrid desalination plant powered by parabolic trough solar collectors that utilized both MSF and RO desalination methods. The goal of this study was to develop a system that can meet the increasing water and energy demands of Egypt. Mathematically models of each component of the proposed system were individually created. The mathematical models were then combined into a MATLAB Simulink model that simulated the entire system. The simulation provided data that was used to perform an economic analysis to compare this system to traditional systems. This study assumed that the plant would be running at optimal performance[16]. This study showed great promise for using a hybrid desalination system. However, multiple factors were not considered, such as brine disposal and the system running at sub-optimal performance. This study showed the potential of using a system that combines thermal and membrane desalination technologies and is powered by renewable energy sources.

2.1.4 Brine Disposal

Brine is highly concentrated saltwater that is a byproduct of most desalination processes. Brine disposal can have a significant negative impact on the marine environment, including the destruction of marine habitats. There are several methods for disposing of brine, including surface water discharge, sewer discharge, deep-well injection, and evaporation ponds.

The most commonly used method for brine disposal is surface water discharge, with over 90% of all saltwater desalination plants using it[17]. Surface water discharge involves releasing brine into nearby bodies of water. Surface water discharge is a cost-effective means of brine disposal, and it can be used for a wide range of plant sizes. However, surface water discharge can harm marine life because it causes an imbalance in salinity and major ions[18]. Additionally, brine with a higher temperature than that of the ambient seawater, such as brine from thermal desalination technologies, can be severally harmful to surrounding marine life[19].

Sewer discharge is another method for disposing of brine that involves mixing it with domestic sewage before discharging it into the sewer system. This method is only suitable for the brine that meets certain water quality standards because if the brine contains harmful chemicals, it can contaminate the sewer system and harm microorganisms, plants, and soil[18].

Deep-well injection involves injecting the brine into deep geological formations, where it can be stored indefinitely. This treatment method can be used for inland treatment plants, but it can potentially contaminate surrounding groundwater, and it is not feasible for areas with lots of seismic activity. Additionally, it requires geological formations that are hydraulically isolated to use for storage, and it is often expensive[18,19].

Evaporation ponds are another method for disposing of brine that involves storing the brine in large ponds and allowing it to evaporate naturally over time. Evaporation ponds are easy to implement and are low maintenance. However, they require a large amount of land, and there is a risk of contaminating the surrounding soil and groundwater[18,19].

Each method for brine disposal has its own advantages and disadvantages, and the appropriate method of disposal depends on the specific characteristics of the brine, such as its salinity, temperature, and chemical composition, as well as the location and availability of infrastructure. The selection of a brine disposal method is critical to the environmental sustainability of a desalination plant. As the demand for freshwater continues to increase, the importance of effective and sustainable brine management will become even more critical. Innovations in zero liquid discharge systems can reduce the environmental impact caused by brine disposal.

2.2 Wave Energy Converters

One issue in every type of desalination is the enormous energy requirements. Wave energy has high energy potential and is one of the most reliable forms of renewable energy, but it is also costly to develop because of the complexity of waves. A WEC is a device that extracts energy from ocean waves and converts it into usable energy. There are three main types of WECs: point absorbers, attenuators, and terminators. Point absorbers are floating devices that move up and down with the motion of waves. Attenuators are long floating structures that are oriented parallel to the direction of wave travel. As waves pass over the attenuator, it bends and flexes, which generates electricity. Terminator WECs are oriented perpendicularly to the direction of wave travel. The WEC used in this research is a type of terminator WEC called an OSWEC, which consists of a fixed base and a flap that oscillates with the motion of the waves. This type of WEC is used because it has the capability to directly pressurize and pump water to the desalination system.

WEC-Sim is an open-source wave energy converter simulation tool developed by the National Renewable Energy Laboratory. WEC-Sim provides the fundamental tools needed for simulating a WEC. It also provides developer tools that make it so other systems can be

attached and simulated with the WEC through MATLAB Simulink[9]. A study was done on how WEC-Sim could be used to evaluate the optimal location for a WEC in the Caspian Sea. This study began by collecting wave data from multiple locations along its southern coast. The wave data was then processed and used to develop an optimal geometry. The geometry of the WEC was modeled using a program called ABAQUS. The hydrodynamics were simulated using a program called NEMOH. The resulting hydrodynamic and geometry models were used to create the simulation of the WEC in WEC-Sim. A sensitivity analysis was conducted using WEC-Sim to optimize the height of the flap for the various locations. For this analysis, three different heights were used for each location. Once the height was optimized, further analysis was done to optimize the PTO damping factor. The total power output and external forces of the optimized WECs were compared to determine the optimal location[20]. This study provides information on how WEC-Sim can optimize a WEC's performance through a sensitivity analysis.

Another study was done on optimizing the hydraulic PTO system for a point absorber WEC in Perth, Australia. The WEC for this study used a buoy to absorb the energy from the waves. A piston used the motion of the float to pressurize and pump hydraulic fluid. The flow out of and into the piston was controlled by rectifying valves. A hydraulic motor uses the hydraulic energy from the piston to rotate a shaft that powers a rotary generator that converts the motion of the rotating shaft into electricity. High- and low-pressure accumulators were connected to either side of the hydraulic motor to reduce the hydraulic fluctuations and provide a more consistent power source. A model of the WEC and hydraulic PTO system was created in WEC-Sim. Three metaheuristic optimization methods and three numerical optimization methods were used to optimize four parameters of the PTO. The parameters investigated were the piston area, high- and low-pressure accumulators, and the low-pressure accumulator pre-charge pressure. A feasibility study of the resulting parameter ranges was conducted through a literature review on similar WECs.

After the feasibility study limited the parameter ranges, a sensitivity analysis was conducted by running the WEC-Sim model over 250 times with varying combinations of parameters. The optimization convergence of ten different algorithms was determined, and then the ten algorithms were compared to each other to determine the best method[21]. This study demonstrates how multiple optimization methods can be used and the value that sensitivity analysis can add to optimizing a WEC and PTO system.

2.3 Wave Powered Desalination

Wave energy converters have a high potential for powering desalination systems. One study performed an economic analysis on the potential use of a wave-powered RO system in the United States[22]. The WEC and the RO desalination systems were modeled in MATLAB using WEC-Sim and Simulink. The simulated model was validated against a small-scale wave tank test. The system analyzed in this study used the WEC to directly pressurize the feed water into the desalination unit. Transmitting the mechanical power of waves to electrical power for transmission and then back to mechanical power used to pressurize water results in many losses that negatively affect the system's efficiency. By directly pressurizing the water, these losses are removed. The formula for levelized cost of energy, also known as LCOE, used by the U.S. Department of Energy was modified to calculate the levelized cost of water or LCOW for short. This calculation makes assumptions about the economic life of the system, inflation rates, tax rates, and discount rates. The resulting LCOW value estimated that the system would be able to produce an average of one cubic meter of water for the cost of about $1.79 USD. This study showed how the LCOW changes as desalination systems are able to produce larger quantities of water[22]. The economic analysis is detailed and provides valuable insight into the cost associated with this type of system and how using a WEC to directly pressurize water can reduce the cost of desalination.

A study was done to develop a numerical model of a wave-to-water desalination system. This model used MATLAB Simulink in association with WEC-Sim to simulate a wave-powered RO system. For this model, the hydrodynamic data of the WEC was obtained using WAMIT, and WEC-Sim was used to model the WEC's reaction to waves over time. A solution-diffusion model was coupled to WEC-Sim in Simulink to develop a wave-to-water model. This developed model uses a wave energy converter that provides mechanical power to a pump that pressurizes seawater and sends it to an RO membrane to produce fresh water. The simulations for the WEC and RO systems were separately validated. The WEC was validated using published experimental data. The RO system was validated using WAVE with the Reverse Osmosis System Analysis (ROSA) feature. The developed model was tested under different wave conditions to evaluate how the pressure and flow rate fluctuation impacts the system's performance. This study showed that fluctuations in wave energy have a large impact on the system and produced water. This study incorporates a pressure-relief valve and accumulator that helps reduce the fluctuations, but the effectiveness of these devices depends on the wave conditions. This type of system can reduce wave-to-wave fluctuations and further increase the performance of the RO membrane. Multiple methods for reducing hydraulic fluctuations are proposed, but each increases the system's price, and trade-offs[23]. This study provides useful information on developing a numerical model for a wave-to-water desalination system using reverse osmosis. However, it does not consider the disposal of brine produced by the system. This thesis will further add to the work done in this study by incorporating SCWD into the system to treat the brine output of the system, and a sensitivity analysis will be performed to optimize the system. Additionally, the work done in this thesis used a rotational PTO, while the above study used a linear hydraulic piston PTO.

Chapter 3

Methodology

3.1 System Overview

The zero-waste wave-to-water desalination system consists of four main subsystems: The WEC, the PTO, the RO system, and the SCWD system. The WEC converts the motion of wave waves into usable mechanical energy. The PTO unit uses the mechanical energy from the OSWEC to pressurize and pump seawater to the desalination system. The pressurized seawater from the PTO is sent to the RO desalination system. An accumulator and pressure relief valve are connected between the PTO and RO subsystems to reduce the hydraulic fluctuations entering the desalination system membrane. Reducing the hydraulic fluctuations going into the membrane increases the performance and extends the life of the membrane. The RO system separates the pressurized seawater into fresh water and brine. The freshwater is collected while the brine is sent to the SCWD system. The SCWD system separates the brine into solid salt and fresh water. Figure 3.1 depicts an overview of the zero-waste wave-to-water desalination system.

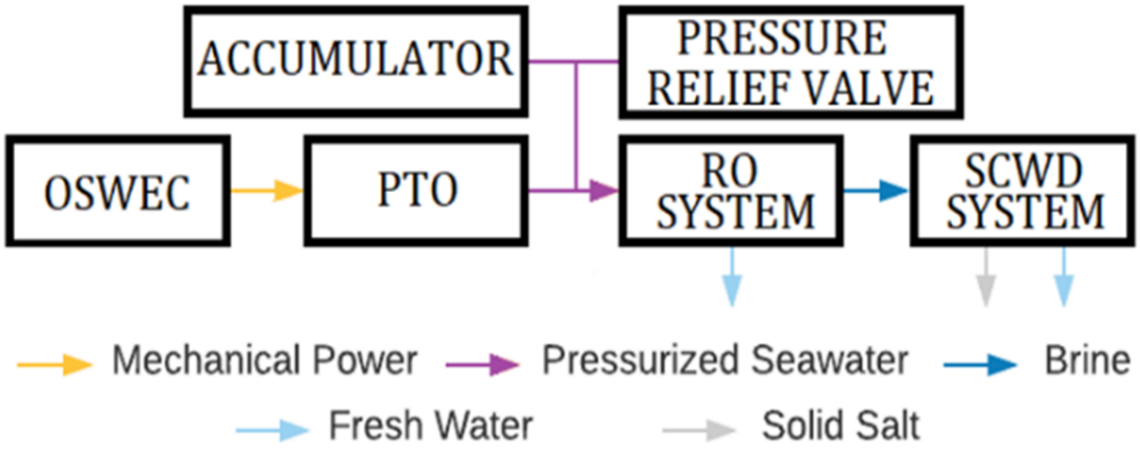

Figure 3.1: Zero-Waste Wave-To-Water Desalination System Overview.

This thesis presents the development of a numerical model for the zero-waste wave-to-water desalination system. The numerical model of the system was developed in MATLAB Simulink. Figure 3.2 shows the overall model for the system. The subsystems for the four main components will be discussed in Sections 3.2 through 3.5. The accumulator was modeled using a gas-charged accumulator block from the Simscape Fluids MATLAB addon. The accumulator volume was one of the parameters tested in the sensitivity analysis, which is discussed further in Section 3.6. The precharge pressure for the accumulator was set as 27 bar, which is 90% of the minimum working pressure for the system. The minimum working pressure for the system was 30 bar, which is the assumed osmotic pressure for the RO membranes and is discussed further in Section 3.4. The pressure relief valve was modeled using a pressure relief valve block. The pressure setting for the pressure relief valve was set as 57 bar, which was selected based on the operational range of the RO membranes[23]. The type of RO membrane is another parameter investigated in the sensitivity analysis. The Simulation Settings subsystem contains a solver configuration block that sets the solver type and sample time for the simulation. Also contained in this subsystem is a custom hydraulic fluid block which sets the fluid type for the system as seawater at a temperature of 20°C.

The Simulation settings subsystem is shown in Figure 3.3

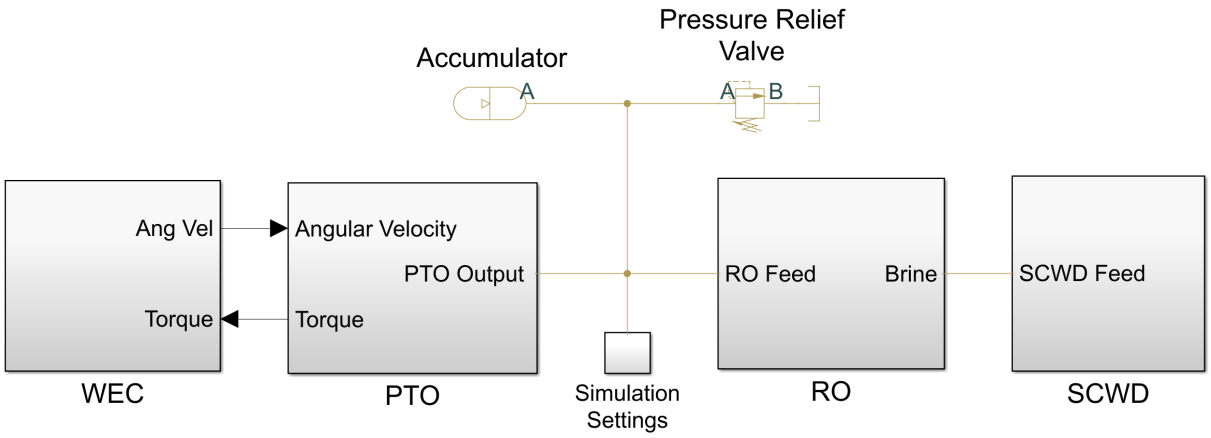

Figure 3.2: Simulink Model Overview.

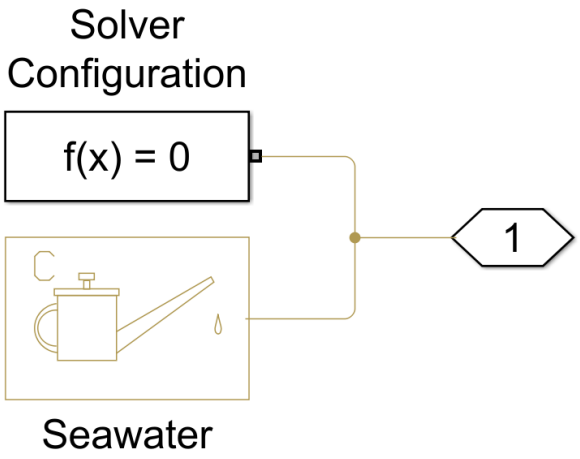

Figure 3.3: Simulink Simulation Setting Subsystem.

3.2 Wave Energy Converter Subsystem

The WEC used in this research was an OSWEC. This type of WEC was used because of its ability to directly pressurize and pump seawater to the desalination system. The WEC subsystem used in this research was a 1:15 scale OSWEC. The scale of the WEC was selected based on the capabilities of a wave tank at the Coastal Studies Institute at Jennette's Pier

on the coast of North Carolina. SolidWorks was used to develop a model of the WEC's geometry. Figure 3.4 shows the SolidWorks model of the WEC used for this research.

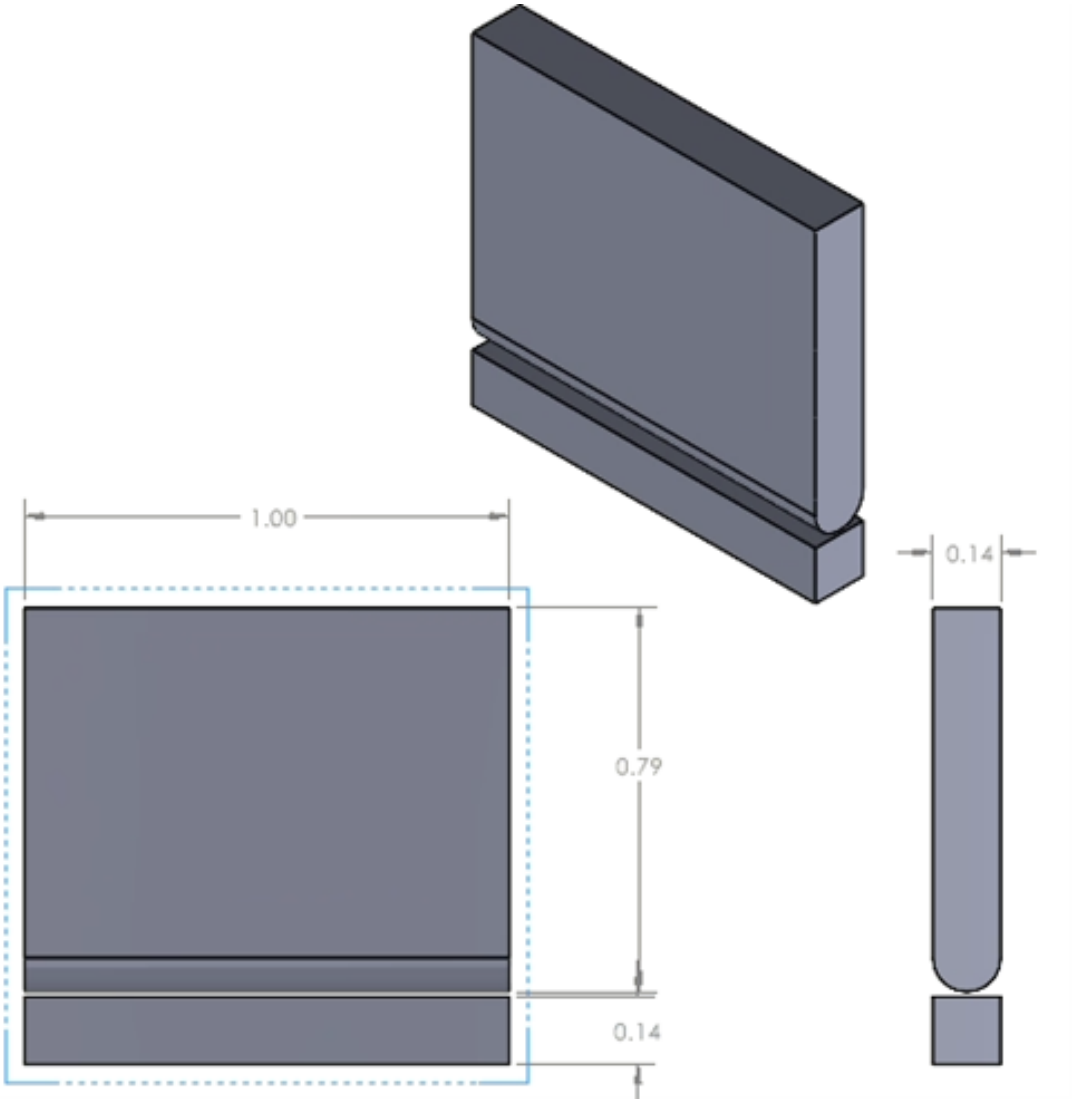

Figure 3.4: Wave Energy Converter SolidWorks Model (Dimensions in Meters)[24].

The small-scale WEC flap was approximately 0.79 m tall, 1.00 m wide, and 0.14 m thick. The base was 0.14 m tall, 1.00 m wide, and 0.14 m thick. Table 3.1 contains the dimensions of the WEC.

Table 3.1: Wave Energy Converter Dimensions

	Width	Height	Thickness
Flap	1.00 m	0.79 m	0.14 m
Base	1.00 m	0.14 m	0.14 m

The SolidWorks model was imported into the Rhinoceros 3D (Rhino) software to generate a quadrilateral mesh of the WEC. SolidWorks is capable of generating triangular meshes, but the quadrilateral meshes generated by Rhino are more accurate compared to the SolidWorks meshes. The mesh generated by Rhino contained 2000 quadrilateral elements. Figure 3.5 shows the quadrilateral mesh for the flap of the WEC. A mesh sensitivity analysis showed that a mesh with 2000 elements or more produced reasonable results[24].

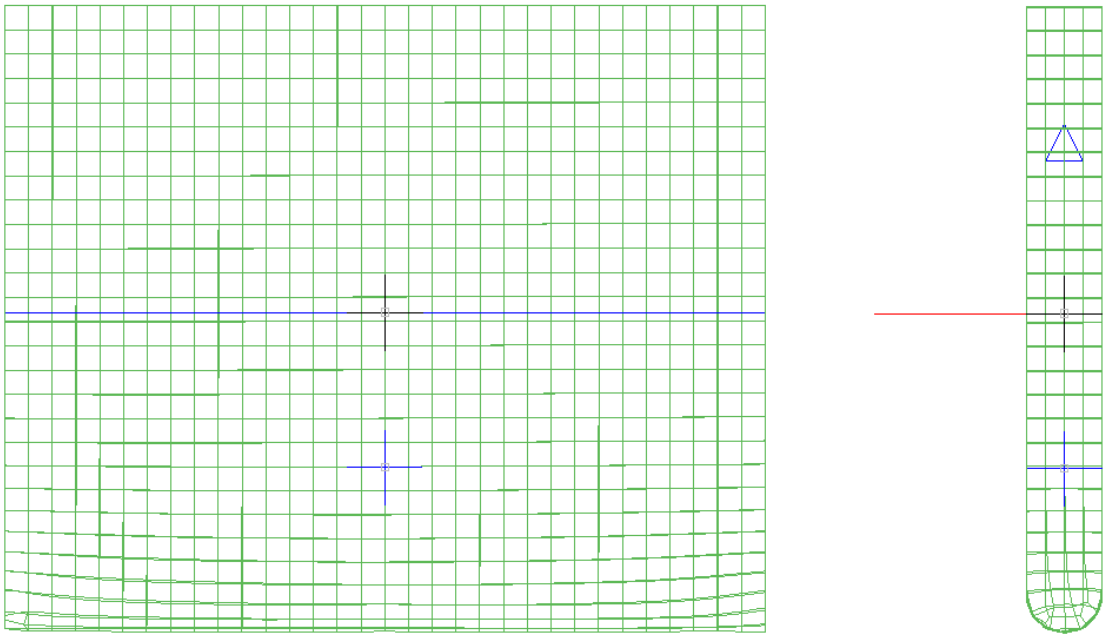

Figure 3.5: Wave Energy Converter Flap Quadrilateral Mesh.

The mesh generated by Rhino was used by a software called WAMIT. WAMIT was used to calculate the hydrodynamic coefficients for the WEC using the boundary integral equation method (BIEM)[25]. The mesh generation and the WAMIT model's development are outside this thesis's scope of work.

The resulting hydrodynamic data from WAMIT was used by WEC-Sim. WEC-Sim provides a Boundary Element Method Input/Output (BEMIO) function that pre-processes the hydrodynamic data for use in the WEC-Sim code. The pre-processing done by BEMIO is explained in-depth on the WEC-Sim website[26]. The pre-processed hydrodynamic data from BEMIO, along with the SolidWorks model, were both used by WEC-Sim to simulate the WEC. The reaction of the WEC to the incident waves and the PTO's force on the WEC was simulated using WEC-Sim. WEC-Sim uses a radiation and diffraction method to determine the hydrodynamic forces from BEMIO to predict the power performance of the WEC and solve the system dynamics in the time domain[27].

The Simulink model for the WEC was made using the WEC-Sim Simulink library. The flap and base of the OSWEC were modeled using rigid body blocks from the WEC-Sim library. A fixed constraint block connected the base to a global reference frame block. A rotational PTO actuation torque block connected the flap to the base. The rotational PTO actuation torque block connects the WEC model to the models of the parts of the system. This block outputs the angular velocity of the WEC to the rest of the system and inputs the torque response from the PTO. Figure 3.6 shows the Simulink model of the WEC.

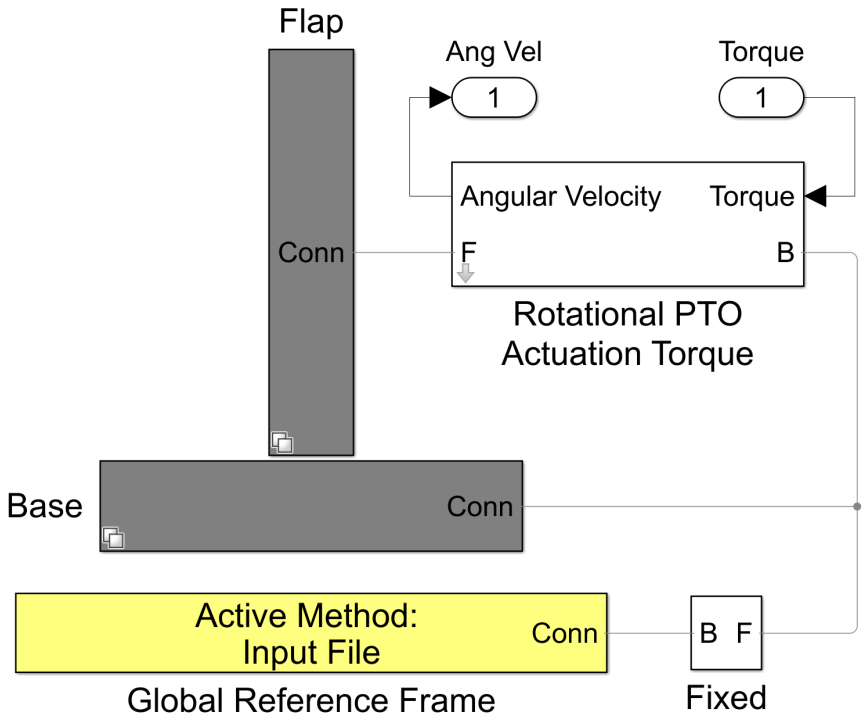

Figure 3.6: Wave Energy Converter Simulink Subsystem.

3.3 Power Take-Off Subsystem

The PTO uses the mechanical energy from the WEC to pressurize and pump seawater to the desalination system. The PTO used in this research consists of a double-acting rotary actuator along with four 2-way/2-position directional control valves. Using a double-acting rotary actuator increased the novelty of the design since current research into wave-to-water desalination systems typically uses a linear hydraulic piston as the PTO. The directional control valves control the flow of seawater from the WEC to the desalination system. The control valves open and close based on the direction of rotation for the WEC so that the pressurized seawater flows out of one chamber to the desalination while unpressurized seawater from the ocean flows into the other chamber.

Figure 3.7 shows the Simulink model for the PTO subsystem. The PTO subsystem uses

the angular velocity from the WEC as an input. It outputs the response torque to the WEC and pressurized seawater to the desalination system. An ideal angular velocity source block converts the angular velocity signal from the WEC to a mechanical rotational domain signal with an angular velocity equal to that of the WEC. The signal from the ideal angular velocity source goes to a double-acting rotary actuator block, which uses this rotation to pressurize and pump seawater into the desalination system. An ideal torque sensor is connected between the rotary actuator and the ideal angular velocity torque to measure the torque response. The measured torque is returned to the WEC subsystem, creating a feedback loop for the angular velocity source block. The rotary actuator has two chambers. As one chamber is being filled, the other is being emptied, which is based on the direction of rotation for the WEC. A relay is used to determine the current direction of rotation, which is then sent to a directional control valve subsystem.

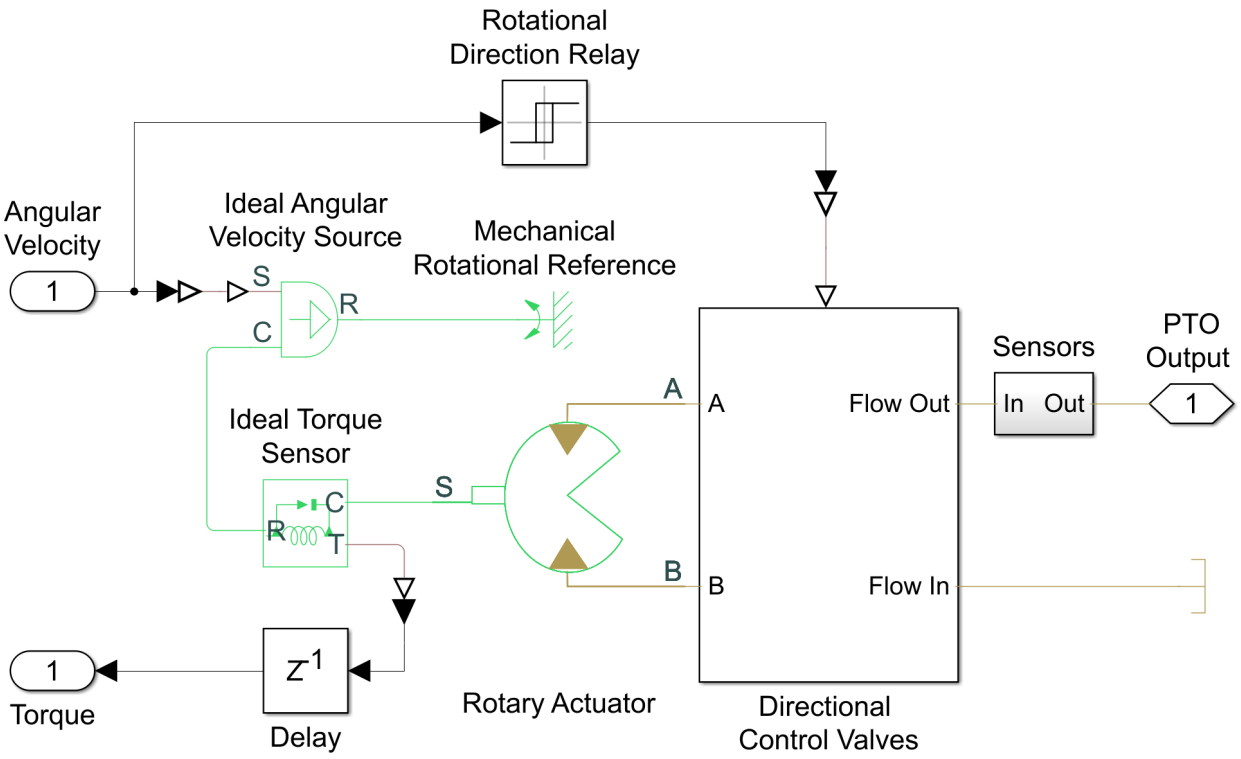

Figure 3.7: Power Take-Off Simulink Subsystem.

The directional control valve subsystem is shown in Figure 3.8. Two 2-way directional valve blocks are connected to each chamber of the rotary actuator. The signal from the relay is directly connected to one of the two directional control valves connected to each chamber, while an inverter is used for the other. This makes it so that when fluid is being pumped out of the chamber, it goes to the desalination system, and when fluid is being pumped into the chamber, it is coming from the ocean. A hydraulic reference port is used to represent the ocean, which is where the directional control valves draw fluid from. A sensor subsystem measures the flow rate and pressure of the fluid exiting the PTO. This subsystem is shown in Figure 3.9, and it contains an ideal pressure sensor and an ideal flow rate sensor.

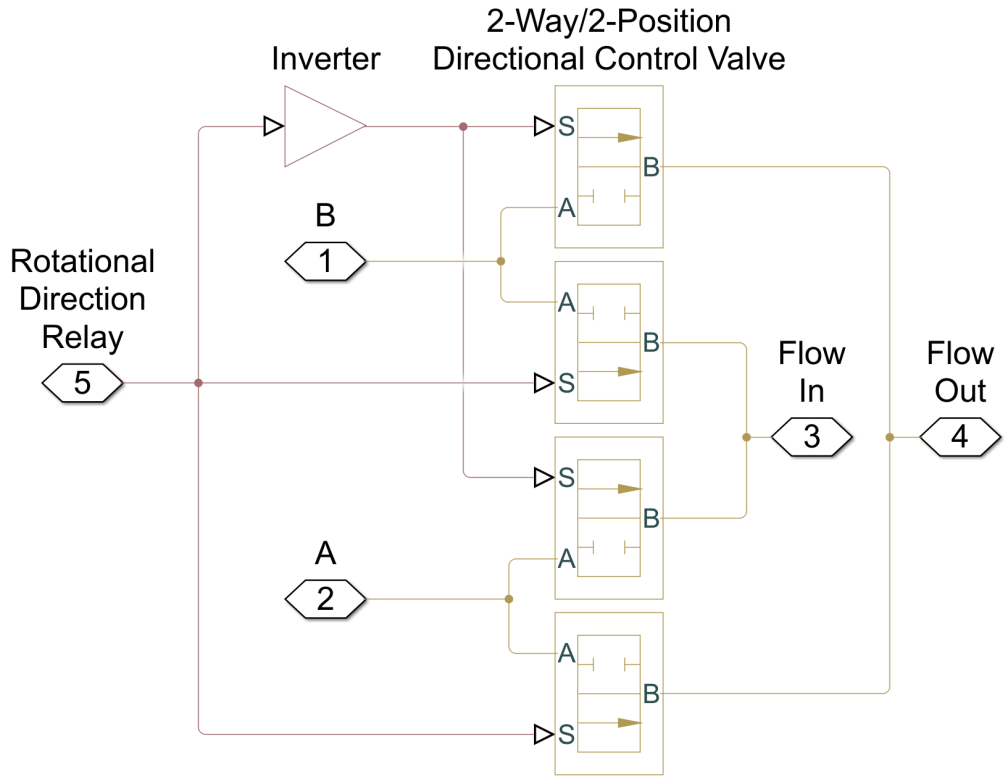

Figure 3.8: Directional Control Valve Simulink Subsystem.

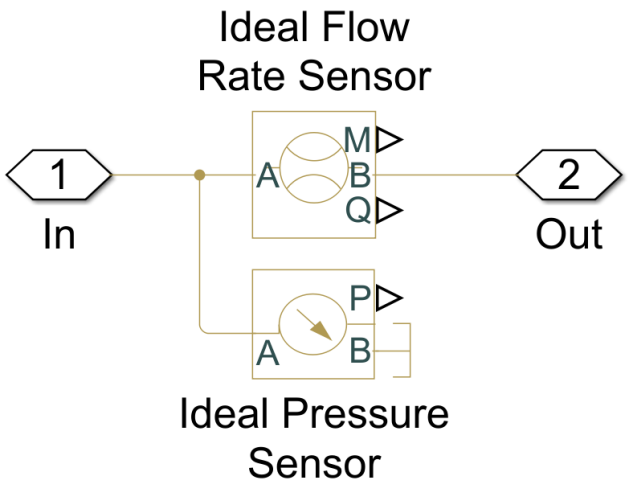

Figure 3.9: Hydraulic Sensors Simulink Subsystem.

3.4 Reverse Osmosis Subsystem

An accumulator and pressure relief valve work together to reduce hydraulic fluctuations and large pressure spikes in the feedwater entering the RO membrane from the PTO. The RO subsystem is based on a model developed by Yu and Jenne[23]. This model uses a solution-diffusion model to simulate the RO process. It assumes that the permeate flow is mainly controlled by the difference between the feed pressure and the osmotic pressure[23]. The solution diffusion model is one of the most widely used methods for modeling reverse osmosis[28].

The Simulink model for the RO subsystem used a pressure relief valve to model the osmotic pressure for the RO process. Osmotic pressure is the minimum pressure required to keep the feed water flowing from the higher concentration side to the lower concentration side. The osmotic pressure for seawater at 25°C typically ranges from 25 to 33 bar[29]. For this model, the osmotic pressure was assumed to be 30 bar[23]. The resistance from the RO membrane was modeled using a linear hydraulic resistor. WAVE is a computer application used for designing and simulating RO systems[30]. Three different membranes were tested during the sensitivity analysis, which will be discussed further in Section 3.6. WAVE was used

to develop models for and simulate each of the membranes used in the sensitivity analysis under multiple different feed pressures ranging from 30 bar to 57 bar. These simulations provided results for the permeate flow rate as a function of the feed pressure, which was used to calculate the resistance for the associated RO membrane. The permeability coefficient of each membrane was calculated using Equation 3.1.

$$A_\omega = \frac{Q_p}{A_m(\Delta p - \Delta\pi)} \tag{3.1}$$

where A_ω is the permeability coefficient, Q_p is the permeate volumetric flow rate, A_m is the membrane active surface area, Δp is the feed pressure, and $\Delta\pi$ is the osmotic pressure. The membrane's active surface area was calculated by multiplying the number of membranes by the area of one membrane. A single membrane was used for this research. The resistance for each membrane was calculated using Equation 3.2.

$$R = \frac{1}{A_m A_{\omega,avg}} \tag{3.2}$$

where R is the membrane resistance, $A_{\omega,avg}$ is the average permeability coefficient, and A_m is the active membrane surface area. Equation 3.3 was used to calculate the solute transport parameter for each of the RO membranes from the WAVE results.

$$B_s = \frac{A_\omega C_p(\Delta p - \Delta\pi)}{C_m - C_p} \tag{3.3}$$

where B_s is the solute transport parameter, C_m is the solute concentration of the water feeding into the membrane, C_p is the solute concentration of the permeate, A_ω is the permeability coefficient, Δp is the feed pressure, and $\Delta\pi$ is the osmotic pressure. The solute transport parameter was used to determine the solute concentration in the permeate water produced by the RO subsystem in the Simulink model. In the Simulink model, the feed water salinity was assumed to be constant at 35,946 ppm, and Equation 3.4 was used to

calculate the solute concentration of the permeate[23].

$$C_p = \frac{C_p}{\frac{A_\omega}{B_s}(\Delta p - \Delta\pi)} \tag{3.4}$$

where C_p is the solute concentration of the permeate, C_m is the solute concentration of the water feeding into the membrane, A_ω is the permeability coefficient, B_s is the solute transport parameters, Δp is the feed pressure, and $\Delta\pi$ is the osmotic pressure. The permeate solute concentration was used to determine the quality of the water produced by the RO subsystem. Table 3.2 provides the relationship between the water quality and the total dissolved solids in the water[31–33].

Table 3.2: Water Quality Based On Total Dissolved Solids (TDS)[31]

Water Quality	Total Dissolved Solids (TDS)
Excellent	<300 ppm
Good	300 ppm - 600 ppm
Fair	600 ppm - 900 ppm
Poor	900 ppm - 1200 ppm
Unacceptable	>1200 ppm

Based on Table 3.2, the desired permeate solute concentration is less than 300 ppm. The U.S. Environmental Protection Agency (EPA) also has a non-enforceable standard for drinking water of 500 ppm[34]. Table 3.3 contains the three different membranes tested in the sensitivity analysis, along with the parameters obtained from the WAVE model for the associated membrane. Figure 3.10 shows the Simulink model for the reverse osmosis subsystem.

Table 3.3: Reverse Osmosis Membrane Parameters

RO Membrane	SW30-2540	SW30-4040	SW30HR-380
Active Membrane Surface Area [m^2]	2.6	7.3	35.3
Permeability Coefficient, A_ω [10^{-12} m^3/Ns]	4.67	4.55	3.45
Membrane Resistance [GPa/(m^3/s)]	82.4	30.1	8.20
Solute Transport Parameter, B_s [10^{-8} m/s]	6.23	3.19	2.13
Minimum Feed Flow Rate, $Q_{F,min}$ [m^3/hr (gpm)]	0.28 (1.23)	1.05 (4.60)	3.97 (17.46)
Maximum Feed Flow Rate, $Q_{F,max}$[m^3/hr (gpm)]	1.4 (6.16)	3.6 (15.85)	14.1 (62.08)

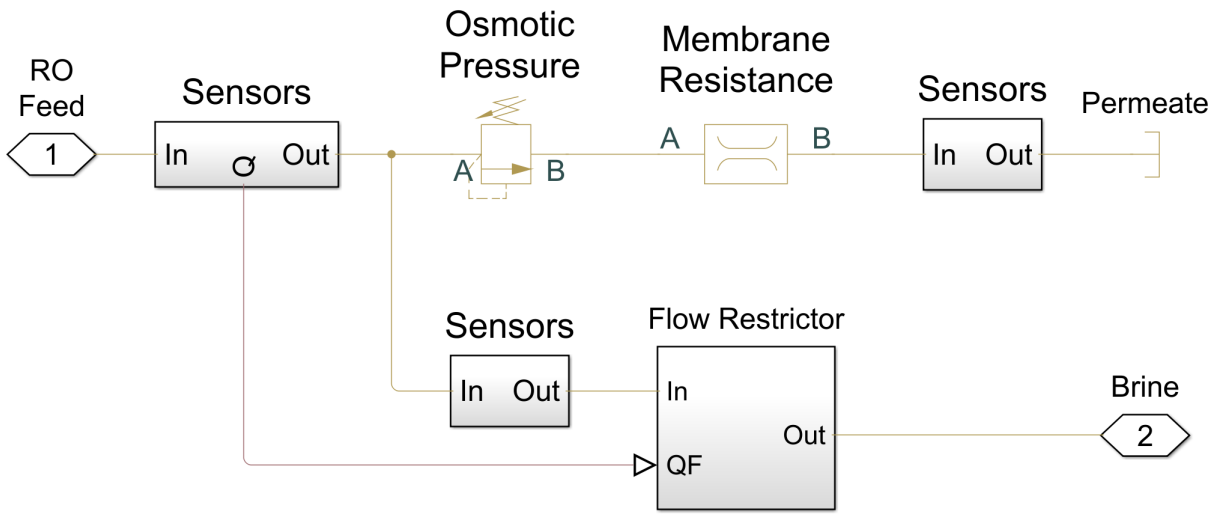

Figure 3.10: Reverse Osmosis Simulink Model.

In reverse osmosis systems, flow restrictors are used to provide back pressure, which makes it so the pressure within the membrane can be maintained[35]. For this reason, a flow restrictor subsystem was added to the brine output of the RO membrane Simulink model. Figure 3.11 shows the Simulink model for the flow restrictor subsystem. In this subsystem, a variable area hydraulic orifice was used to model the flow restrictor. A linear hydraulic resistor was initially used as the flow restrictor since that is what traditional systems use. However, traditional reverse osmosis systems also use a constant flow rate feeding into the membrane, which is not the case in this research. Using a linear hydraulic resistor with this system resulted in issues with the recovery ratio for the RO membrane not being within the recommended limits. Using a variable area flow restrictor instead made it so that the reverse osmosis system could better respond to changes in feed flow rate, and a target recovery ratio could be specified and maintained. For this research, 12.5% was used for the target recovery ratio. This percent recovery was used because it is slightly below the maximum recovery ratio for a single membrane recommended by WAVE, which was 13%. Figure 3.11 shows the Simulink model for the flow restrictor subsystem.

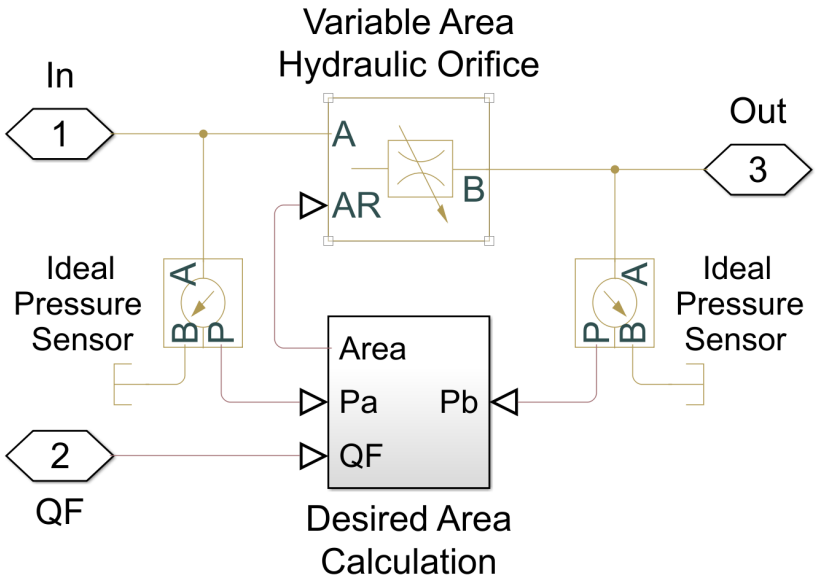

Figure 3.11: Flow Restrictor Simulink Subsystem.

The variable area hydraulic orifice required the area as an input, which was calculated in a subsystem using the target percent recovery, $\%R$, feed flow rate into the membrane, Q_F, the pressure at the inlet of the flow restrictor, $P_{a,FR}$, and the pressure at the outlet of the flow restrictor, $P_{b,FR}$. In this subsystem, the area was calculated using Equation 3.5, which was obtained from the equations provided on the MATLAB help page for the variable area hydraulic orifice block[36].

$$A_{FR} = Q_{Target}\sqrt{\frac{\rho}{2}}\left(\frac{((P_{a,FR} - P_{b,FR})^2 + P_{cr}^2)^{\frac{1}{4}}}{(P_{a,FR} - P_{b,FR})}\right) \tag{3.5}$$

where A_{FR} is the desired flow restrictor area, Q_{Target} is the Target flow rate, ρ is the fluid density, $P_{a,FR}$ is the inlet pressure, $P_{b,FR}$ is the outlet pressure, and P_{cr} is the minimum pressure for turbulent flow during the transition from laminar to turbulent regime[36]. The Target flow rate was calculated using Equation 3.6.

$$Q_{Target} = Q_F(1 - \%R) \tag{3.6}$$

where Q_{Target} is the Target flow rate, Q_F is the feed flow rate going into the membrane, and $\%R$ is the Target recovery ratio. P_{cr} was calculate using Equation 3.7.

$$P_{cr} = (P_{avg,FR} + P_{atm})(1 - B_{lam}) \tag{3.7}$$

where P_{cr} is the minimum pressure for turbulent flow during the transition from laminar to the turbulent regime, $P_{avg,FR}$ is the average pressure between the inlet and outlet pressure, P_{atm} is the atmospheric pressure, and B_{lam} is the pressure ratio at the laminar and turbulent transition point[36]. P_{atm} was set as 101325 Pa, and B_{lam} was set as the default value for the variable area hydraulic orifice block, which is 0.999. $P_{avg,FR}$ was calculated by summing $P_{a,FR}$ and $P_{b,FR}$, and then dividing by 2. Figure 3.12 shows the Simulink model for the area calculation.

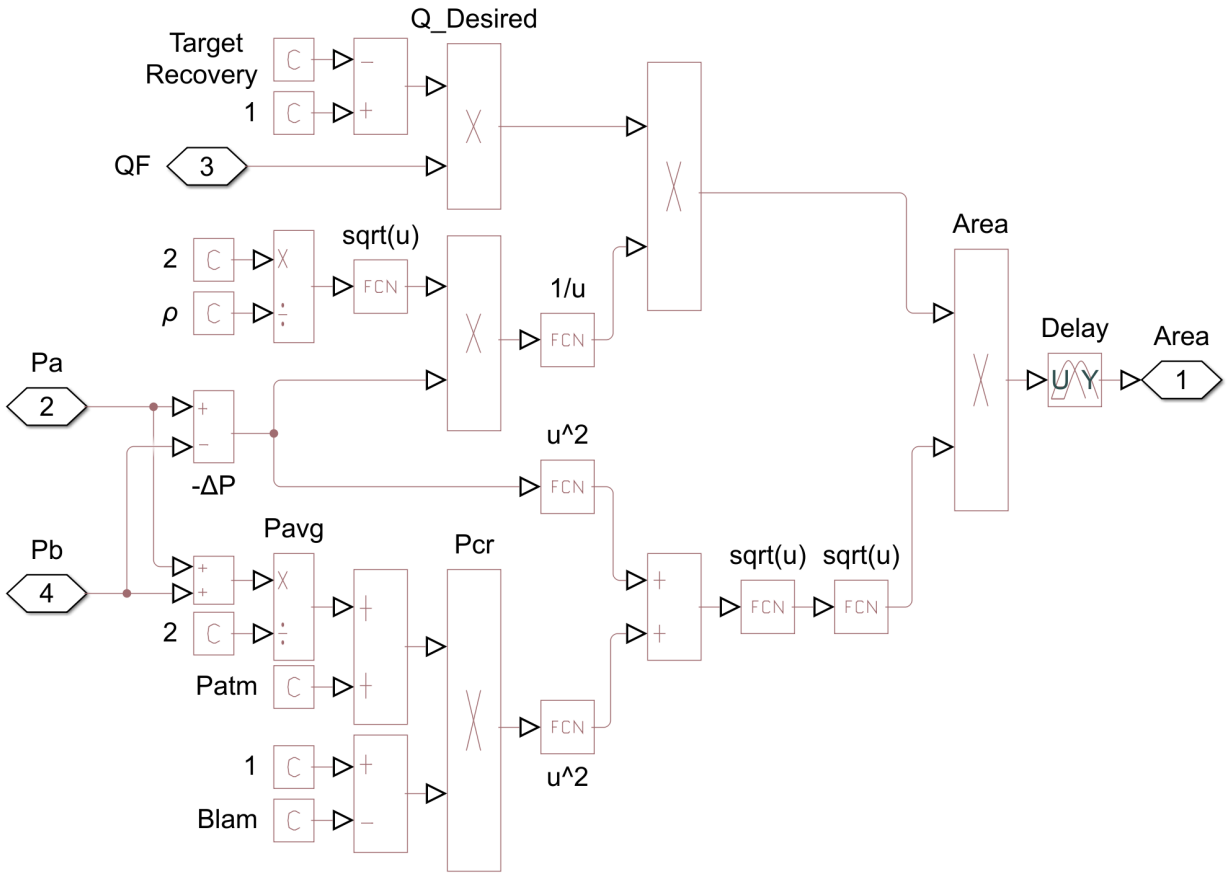

Figure 3.12: Flow Restrictor Area Calculation Simulink Subsystem.

3.5 Supercritical Water Desalination Subsystem

The Simulink model for the SCWD subsystem was a modified version of a model developed by Dr. Jinbo Chen from East Carolina University[37]. The SCWD system used in this research was a two-stage process that consisted of a pump, a heat exchanger, a furnace, two main reactors, and a condenser. Figure 3.13 shows a diagram of the system[37]. The SCWD system used the brine from the RO system as an input. The brine was pressurized by a pump to supercritical pressure conditions. A heat exchanger and a furnace were used to heat the brine to approximately 250°C. The brine then entered the first reactor, which heated the brine to supercritical temperature conditions and then separated the brine into vapor and

liquid forms. The vapor then went through a condenser to produce fresh water that was free of salt. The liquid from the first reactor contained most of the salt (99.9%). This liquid entered the second reactor, which started the flashing process. The flashing process converted the liquid into solid salt mist and water vapor.

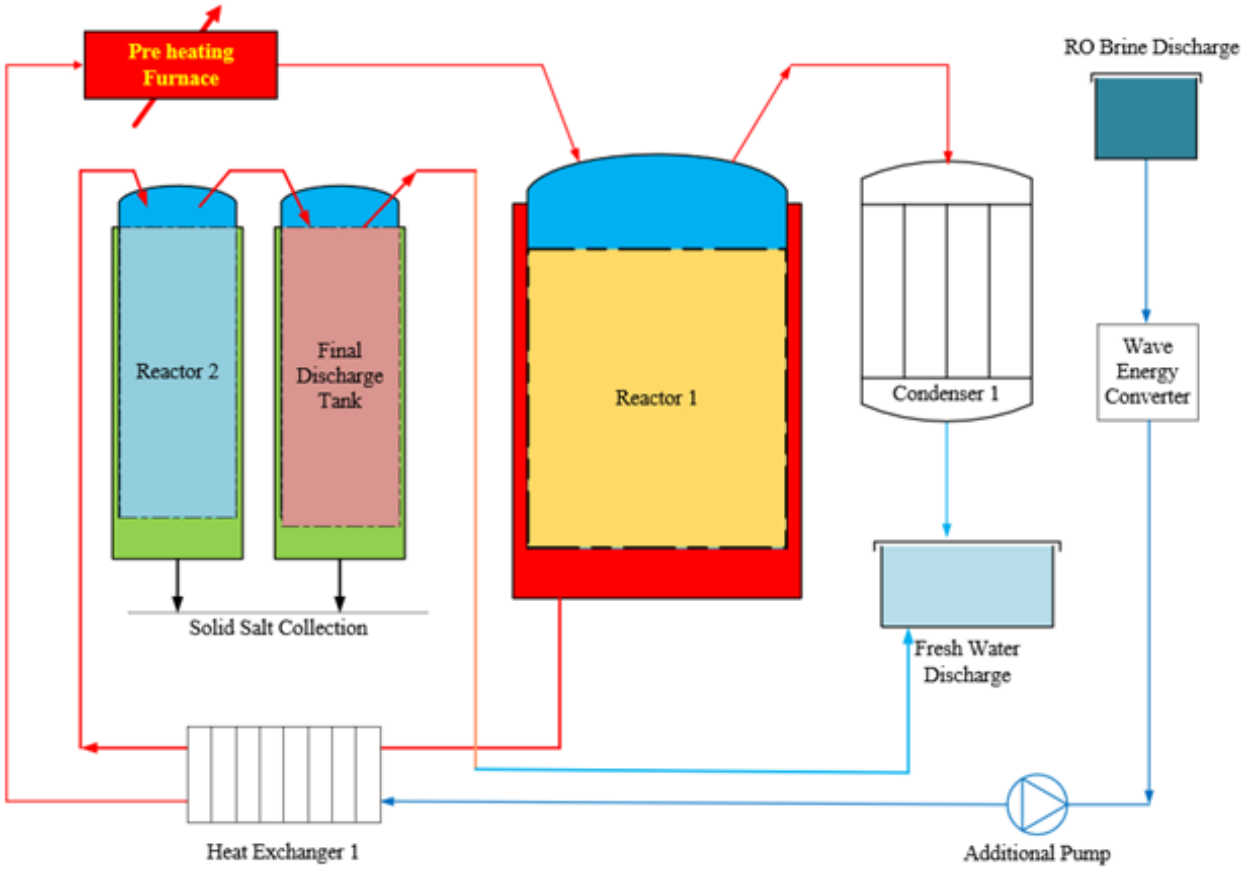

Figure 3.13: Supercritical Water Desalination System Diagram[37].

The SCWD model developed was validated using experimental results. The experimental apparatus is described in[24]. In the Simulink model for the SCWD subsystem used in this research, ideal pressure and flow rate sensors were used to measure the pressure and flow rate entering the subsystem. These sensors were used to convert the Simscape fluids signal to a Simulink signal. The temperature of the feed water was assumed to be 20°C, and the mass weight was assumed to be constant at 7.5%. Assuming a constant mass weight significantly

increased the computational efficiency of the model. The Simulink model for the SCWD subsystem is shown in Figure 3.14.

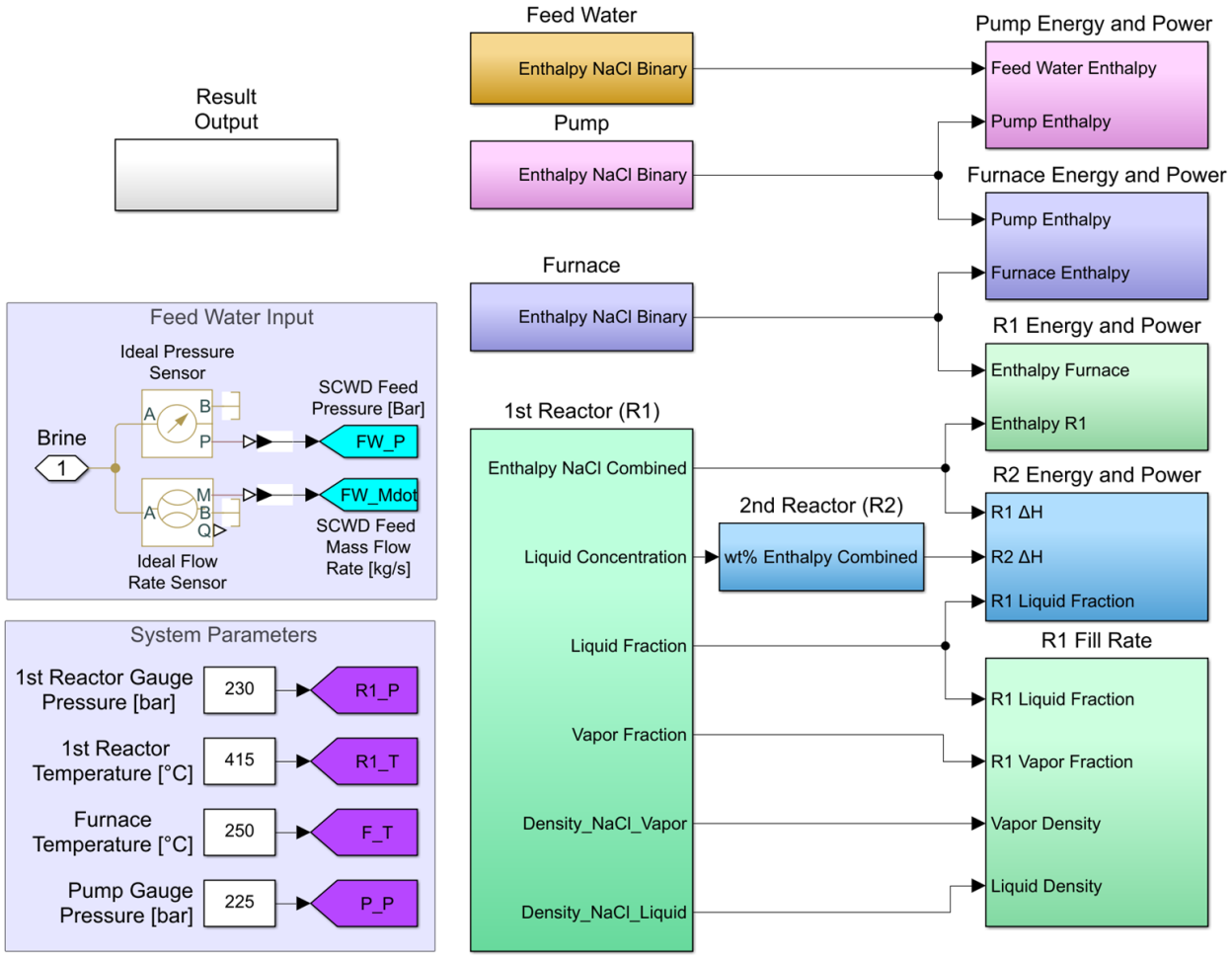

Figure 3.14: Supercritical Water Desalination Simulink Model.

The Reference Fluid Thermodynamic and Transport Properties Database (REFPROP) software was used to determine the feed water enthalpy, as well as the enthalpies of the pump and furnace. The pump operated at a pressure of 225 bar and a temperature of 20°C, while the furnace operated at a pressure of 225 bar and a temperature of 250°C. For the first and second reactors, REFPROP was used in conjunction with a series of equations to calculate the salt removal percentage, along with the liquid and vapor enthalpies, concentrations, specific heats, densities, and fractions. The first reactor operated at a pressure of 230 bar

and a temperature of 415°C, and a feed mass weight of 7.5%. The second reactor operated at a pressure of 220 bar, a temperature of 415°C, and the feed mass weight was set as the liquid concentration from the first reactor.

The energy requirement for the pump was calculated by subtracting the pump enthalpy from the feed water enthalpy. The energy requirement for the furnace was calculated by subtracting the pump enthalpy from the furnace enthalpy. The energy requirement for the first reactor was calculated by subtracting the first reactor enthalpy from the furnace enthalpy. The energy requirement for the second reactor was calculated by subtracting the second reactor enthalpy from the first reactor enthalpy. The power requirement for the pump, furnace, and first reactor was calculated by multiplying the energy requirement by the feed flow rate. The power requirement for the second reactor was calculated by multiplying the energy requirement by the feed flow rate multiplied by the liquid fraction from the first reactor. The total energy and power requirement for the SCWD system was calculated by summing the components' individual energy and power requirements. The vapor production rate for the first reactor was calculated by multiplying the vapor fraction from the first reactor by the feed mass flow rate and then dividing it by the vapor density. Likewise, the vapor production rate for the second reactor was calculated by multiplying the vapor fraction from the second reactor by the feed flow rate multiplied by the liquid fraction from the first reactor. The resulting data was then sent to the MATLAB Workspace to be saved and analyzed.

3.6 Sensitivity Analysis

A sensitivity analysis was performed on the numerical model of the 1:15 scale zero-waste wave-to-water desalination system in order to determine the optimal combination of key system parameters. The sensitivity analysis was conducted using an irregular wave pattern

with a significant wave height of 0.117 m and a peak period of 1.68 s. These wave conditions were selected based on the capabilities of a wave tank at the Coastal Studies Institute at Jennette's Pier on the coast of North Carolina. Figure 3.15 shows a plot of the wave used for the sensitivity analysis.

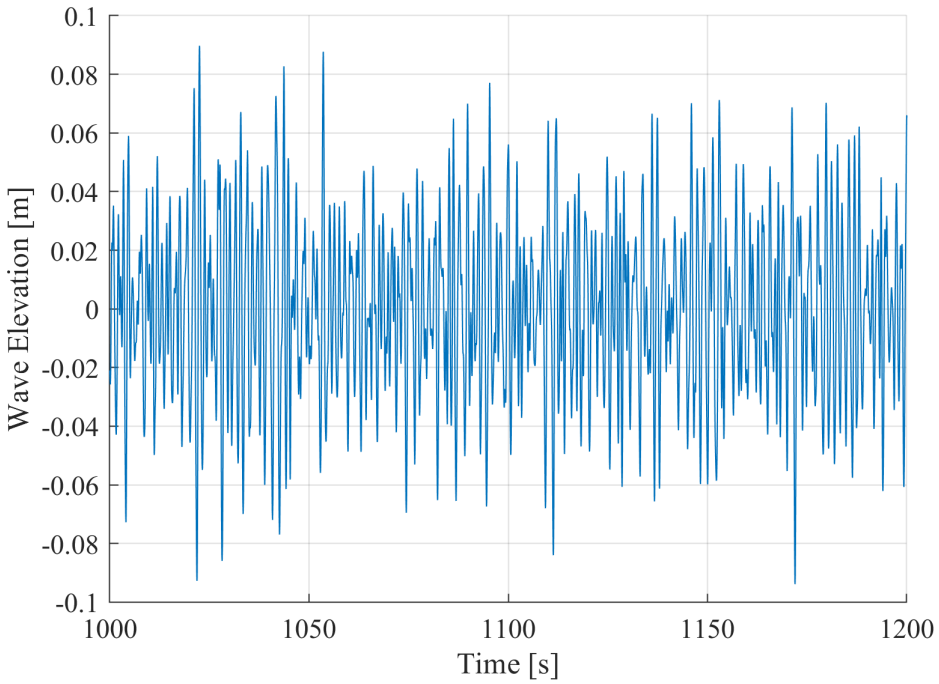

Figure 3.15: Wave Elevation.

The parameters investigated in the sensitivity analysis were the PTO volumetric displacement, the accumulator volume, and the type of RO membrane. The accumulator volume was selected as a key parameter based on the paper written by Yu and Jenne[23]. The type of RO membrane was selected as a key parameter for the sensitivity analysis since each type of membrane has a different range of operating conditions. The PTO volumetric displacement was selected as a key parameter because it affects the volumetric flow rate entering the PTO and the torque going back to the WEC.

Eight different PTO volumetric displacements, three different accumulator volumes, and three different types of RO membranes were used in the sensitivity analysis. The PTO

volumetric displacements were selected based on Micromatic's MPJ double-acting rotary actuators, which are commercially available double-acting rotary actuators. The selected RO membranes were the three smallest membranes in WAVE that could be used for saltwater desalination. The accumulator volumes selected were based on commercially available accumulators. Table 3.4 contains the parameters tested in the sensitivity analysis.

Table 3.4: Sensitivity Analysis Parameters

PTO Volumetric Displacement [cm^3/rad]	Accumulator Volume [gal]	RO Membrane
13.36	2.5	SW30-2540
30.81	5	SW30-4040
61.31	10	SW30HR-380
179		
428		
850		
1386		
1975		

All 72 possible combinations of the parameters in Table 3.4 were tested in the sensitivity analysis. A specific combination of parameters will be referred to as a case (e.g., case 1 was using a PTO displacement of 13.36 cm^3/rad, a 2.5-gallon accumulator volume, and the SW30-2540 RO membrane). The sensitivity analysis was performed using WEC-Sim's multiple condition run (MCR) function. A MATLAB script was used to save the desired results from each case.

A custom MATLAB application was created to view and analyze the results from the sensitivity analysis. This application allowed the user to select the file containing the desired results. The user could then select which result variable was being plotted and which parameters from Table 3.4 to include in the plot. The application would then plot the selected result for each of the selected cases on two separate axes. The primary axis would display the full-time range simulated, while the second axis would plot a small portion of the time.

The time range plotted in the secondary axis could be modified by changing a setting to the side of the plot. The units used for either axis could be modified using a dropdown menu to the side of the plots. Figure 3.16 shows an image of the plot settings and the plot screens for the developed MATLAB application. Under the parameter selection for the RO membrane types, a setting could be used to display horizontal lines on the plots that showed the operational limits for each of the associated RO membrane types. The app could also display a result summary bar graph that would show the operational range of the result variable plotted for each of the selected cases. Next to the bar graph was a table that showed the minimum, maximum, and average values for each case. The result summary screen and the parameter selection screen for the RO membrane are shown in Figure 3.17.

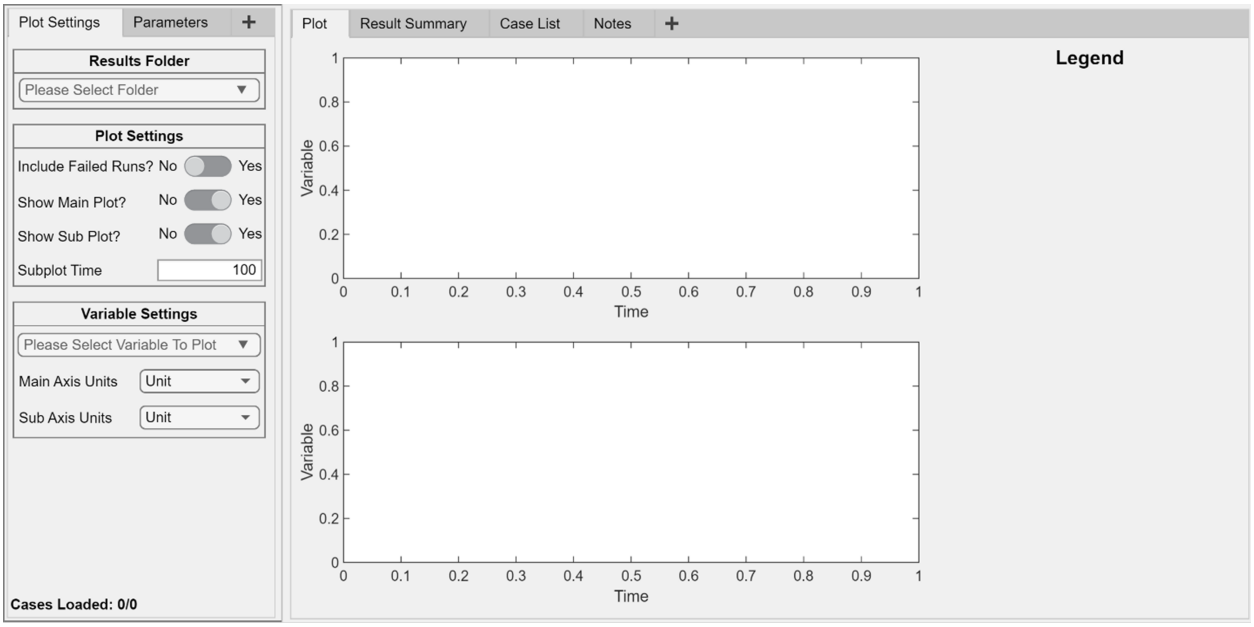

Figure 3.16: Custom Result Analysis MATLAB Application Plot Settings and Plot Screens.

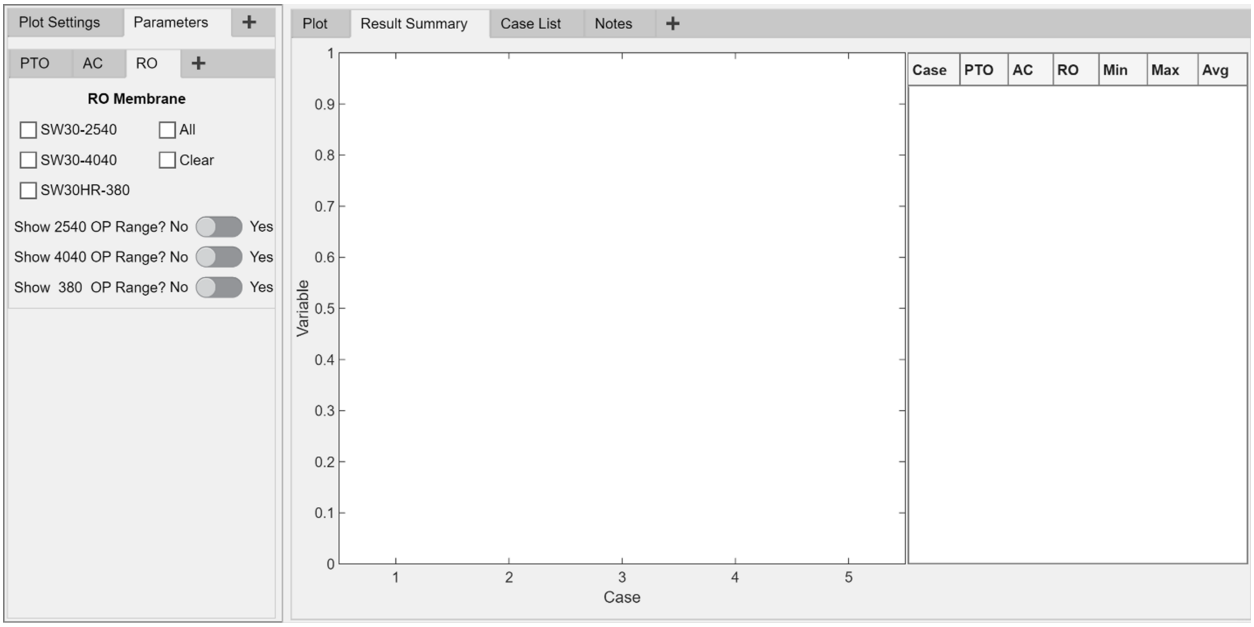

Figure 3.17: Custom Result Analysis MATLAB Application Parameter Selection and Result Summary Screens.

Chapter 4

Results and Analysis

The results of the sensitivity analysis are presented in this section. A total of 72 cases were tested for the 1:15 scale zero-waste wave-to-water desalination system using an irregular wave pattern with a significant wave height of 0.117 m and a peak period of 1.68 s. Only 27 cases of the 72 tested were capable of meeting the pressure and flow rate requirements of RO membrane for the associated case. The permeate flow from the RO system was the primary variable of interest in this sensitivity analysis. This was because water produced by the RO system is cheaper than water produced by the SCWD system. Thus, maximizing the permeate flow rate while maintaining the required pressure and flow rate for the associated RO membrane is crucial in designing an efficient zero-waste wave-to-water desalination system. The amount of hydraulic fluctuations entering the RO system was another factor considered in the sensitivity analysis. This was because larger hydraulic fluctuations can result in a decreased membrane lifespan. Another factor considered was the quality of the produced water. The SCWD requires a large amount of power, so it can require a tremendous amount of power to desalinate a large amount of brine. The effect of each system parameter tested in the sensitivity analysis is discussed in Sections 4.1 - 4.3. Section 4.4 discusses the top three optimal cases.

4.1 Effect of Accumulator Volume on The System's Performance

The accumulator volume had a minimal effect on the amount of water produced by the system. However, the accumulator volume did affect the hydraulic fluctuations entering the RO membrane, which was the primary purpose of the accumulator. In every case, the larger the accumulator volume was, the more the fluctuations entering the RO system were reduced, and the more beneficial the accumulator was to the system. Decreasing the hydraulic fluctuations entering the membrane increases the performance and lifespan of the membrane. Figure 4.1 shows the accumulator volume effect on the feed flow rate entering the RO system with a PTO displacement of 850 cm^3/rad and an SW30-4040 RO membrane.

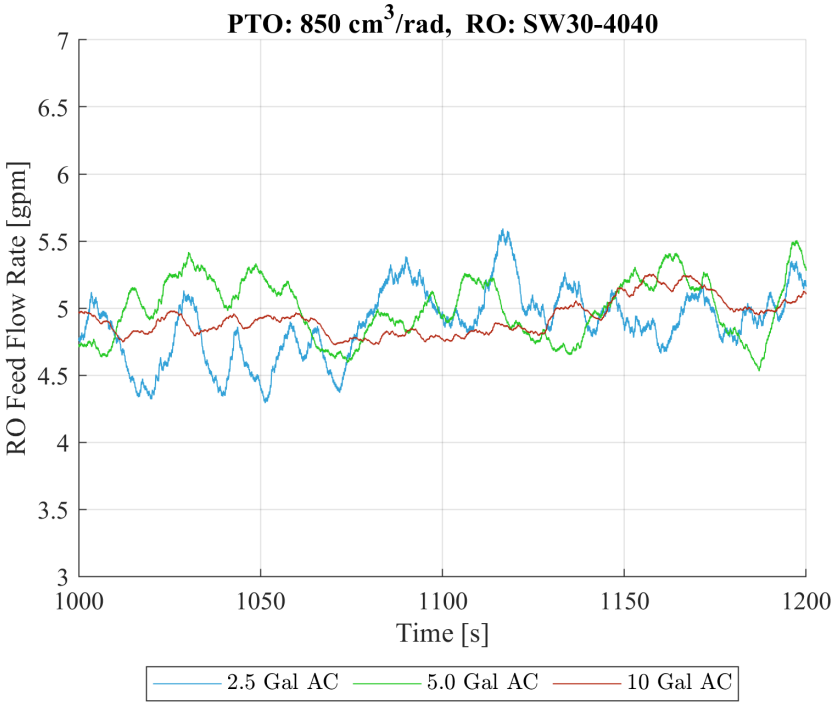

Figure 4.1: Accumulators Effect on the RO Feed Water Flow Rate.

In Figure 4.1, the standard deviation shows that the hydraulic fluctuations for the feed flow rate into the membrane are being reduced. The standard deviations for the RO feed flow

rates are 0.260, 0.225, and 0.133 gpm for the cases with an accumulator volume of 2.5, 5, and 10 gallons, respectively. Figure 4.2 shows the accumulator volume effect on the feed pressures entering the RO system with a PTO displacement of 850 cm^3/rad and an SW30-4040 RO membrane. In Figure 4.2, the standard deviation shows that the hydraulic fluctuations for the feed flow rate into the RO membrane are being reduced. The standard deviations for the feed pressure are 0.619, 0.535, and 0.315 bar for the cases with an accumulator volume of 2.5, 5, and 10 gallons, respectively. Figure 4.3 shows the accumulator's effect on the permeate solute concentration. The standard deviations for the permeate solute concentrations are 11.742, 10.970, and 6.809 ppm for the cases with an accumulator volume of 2.5, 5, and 10 gallons, respectively.

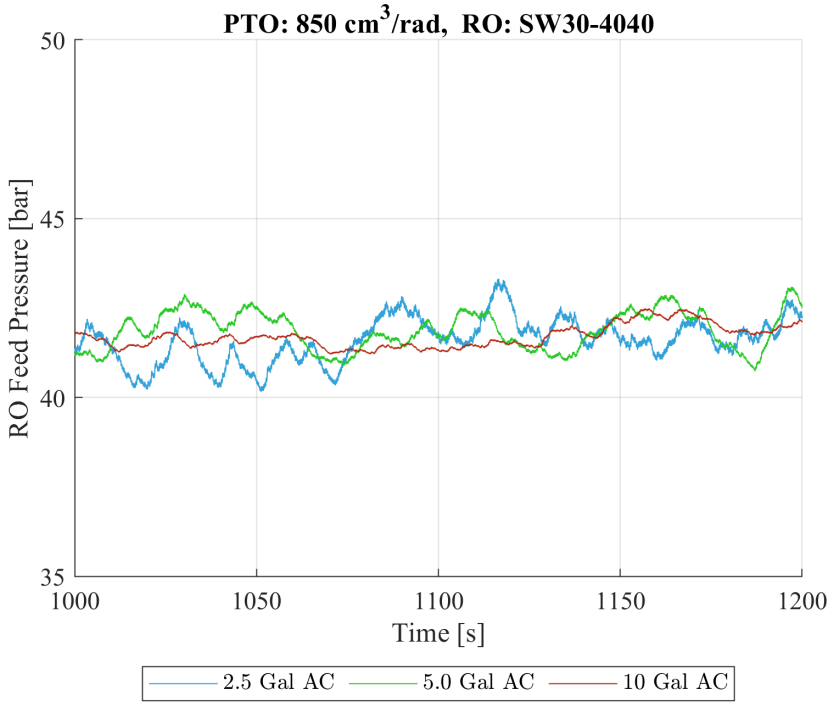

Figure 4.2: Accumulator's Effect on the RO Feed Pressure.

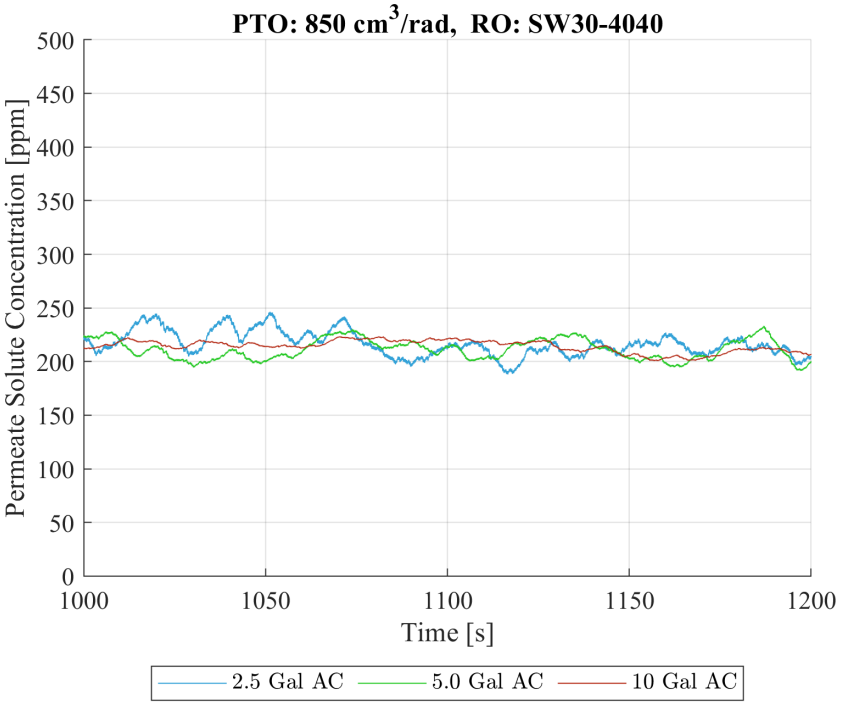

Figure 4.3: Accumulator's Effect on the Permeate Solute Concentration.

4.2 Effect of Reverse Osmosis Membrane Type on The System's Performance

The type of RO membrane significantly affected on the system's performance. The larger the RO membrane was, the more water could permeate through the membrane. However, larger membranes were able to work with fewer PTOs since the PTOs were not able to reach the required pressure and flow rates for the associated membrane. The largest membrane tested in the sensitivity analysis was the SW30HR-380. The SW30HR-380 membrane only worked with the largest PTO volumetric displacement tested, which was 1975 cm^3/rad. The SW30-4040 membrane worked with the three largest PTO sizes, and the SW30-2540 membrane worked with the five largest PTOs out of the eight tested. Figure 4.4 shows a plot of the permeate flow rate for a system with a PTO volumetric displacement of 1975 cm^3/rad, a 10-gallon accumulator volume.

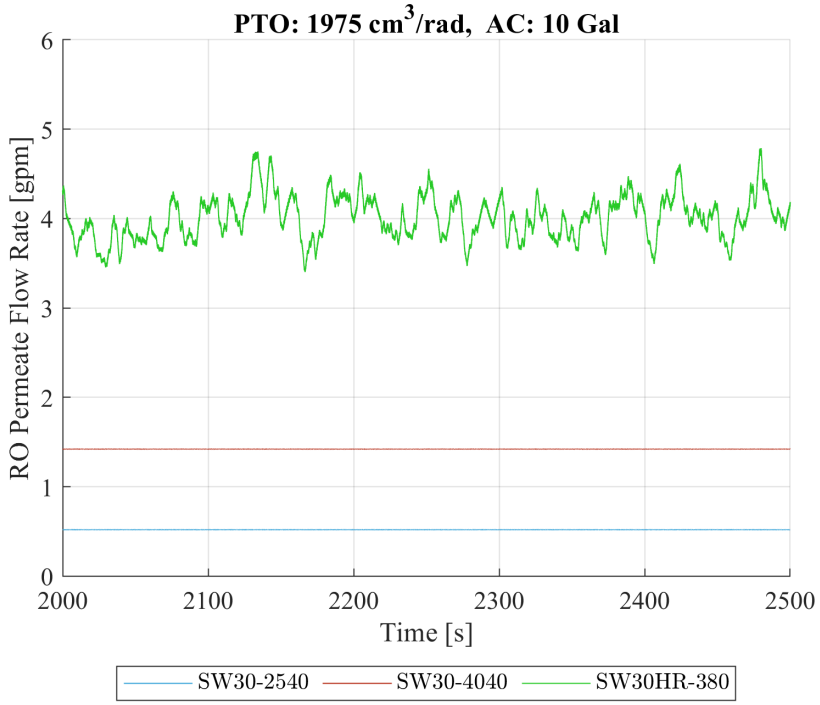

Figure 4.4: The Effect of the RO Membrane Type on The Permeate Flow Rate.

As shown in Figure 4.4, the permeate flow rate was constant for the cases with the SW30-2540 and SW30-4040 membranes with a PTO displacement of 1975 cm^3/rad and a 10-gallon accumulator volume. This was caused by the pressure for the water feeding into the RO system reaching the maximum pressure set by the pressure relief valve, which is shown in Figure 4.5. When the system was operating at the maximum RO feed pressure, additional membranes could potentially be added to increase the recovery ratio of the system and reduce the energy losses from the pressurized seawater exiting the pressure relief valve. Figure 4.6 shows a plot of the permeate solute concentration for each type of membrane using the 1975 cm^3/rad PTO displacement and 10-gallon accumulator.

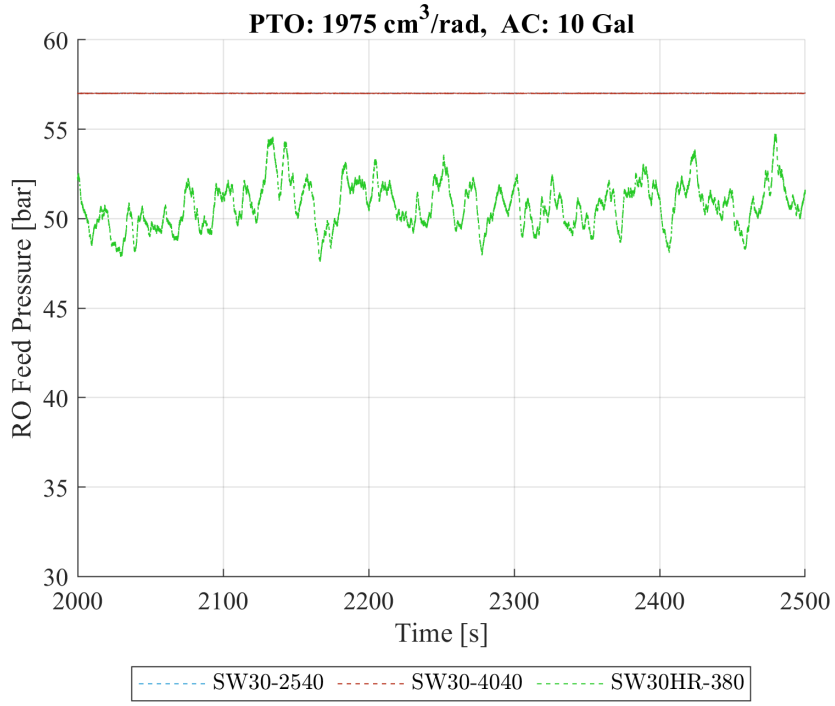

Figure 4.5: The Effect of the RO Membrane Type on The RO Feed Pressure.

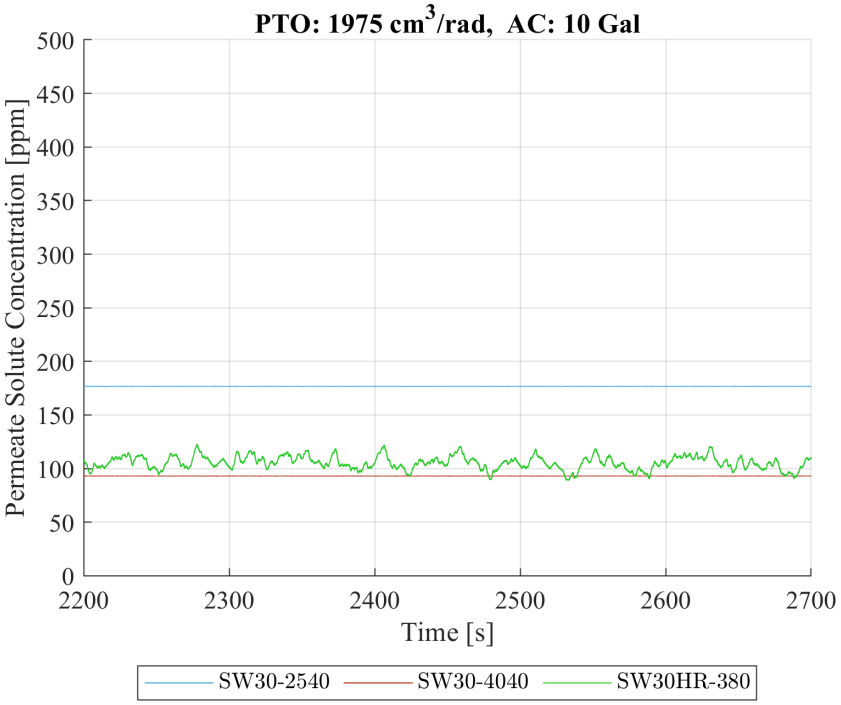

Figure 4.6: The Effect of the RO Membrane Type on The Permeate Solute Concentration.

4.3 Effect of The Power Take-Off Volumetric Displacement on The System's Performance

The PTO volumetric displacement significantly impacted the system's performance. Larger PTO sizes were able to be used with larger RO membranes, which resulted in more fresh water produced by the RO system. The cases that had PTO displacements of 13.36 cm^3/rad, 30.81 cm^3/rad, and 61.31 cm^3/rad were not able to reach the flow rate and pressure requirements for any of the systems. The cases that had PTO displacements of 179 cm^3/rad and 428 cm^3/rad worked only for the SW30-2540 membrane. The cases that had a PTO displacement of 850 cm^3/rad and 1386 cm^3/rad were able to meet the requirements for both the SW30-2540 and SW30-4040 RO membranes. Lastly, the cases that had a PTO displacement of 1975 cm^3/rad worked for all the tested RO membranes. Figure 4.7 shows the PTO volumetric displacement effect on the feed flow rate for a system with an SW30-4040 RO membrane and a 10-gallon accumulator volume. Figure 4.8 shows a plot of the PTO volumetric displacement's effect on the RO feed pressure. Figure 4.9 shows a plot of the PTO volumetric displacement's effect on the permeate solute concentration.

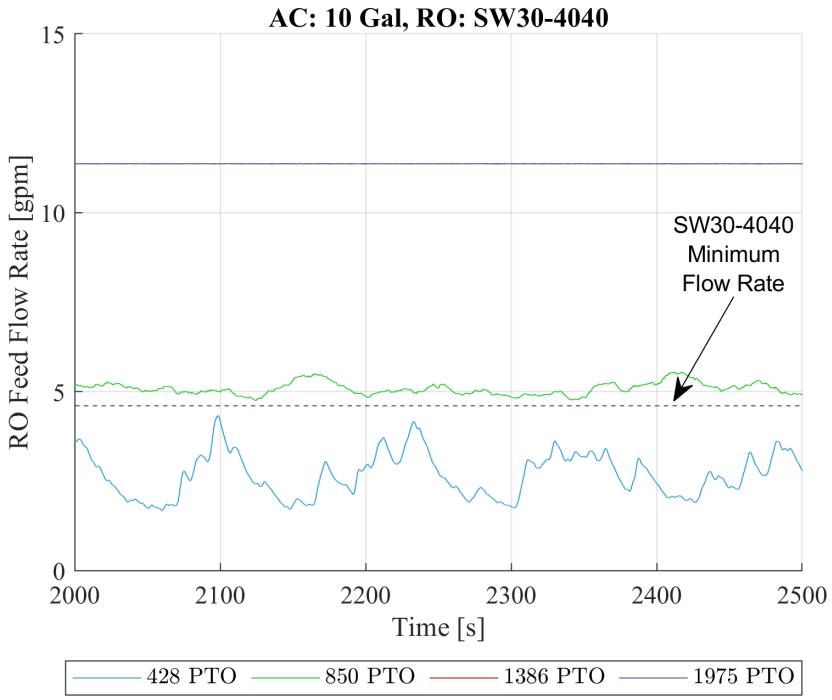

Figure 4.7: The Effect of the PTO Volumetric Displacement on The RO Feed Flow Rate.

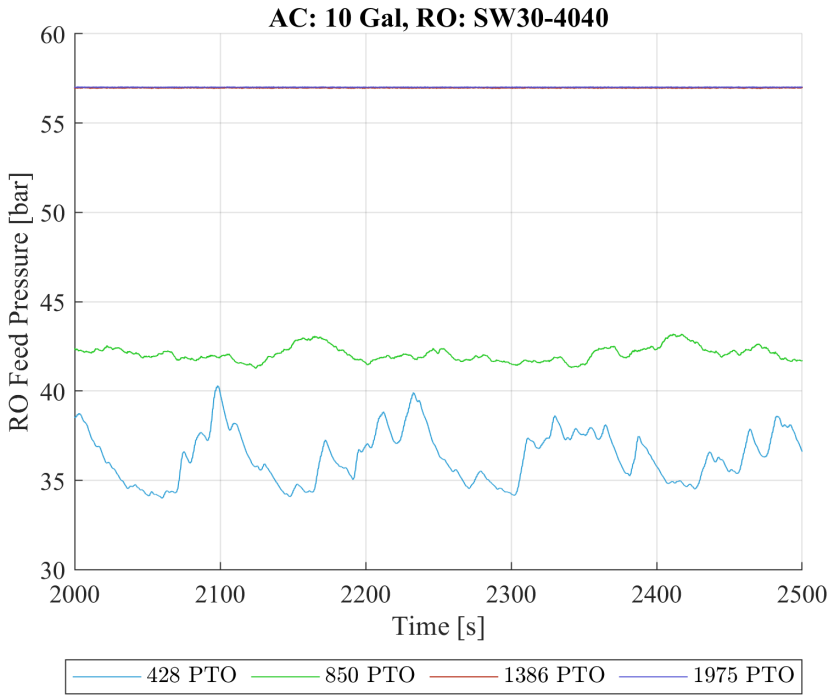

Figure 4.8: The Effect of the PTO Volumetric Displacement on The RO Feed Pressure.

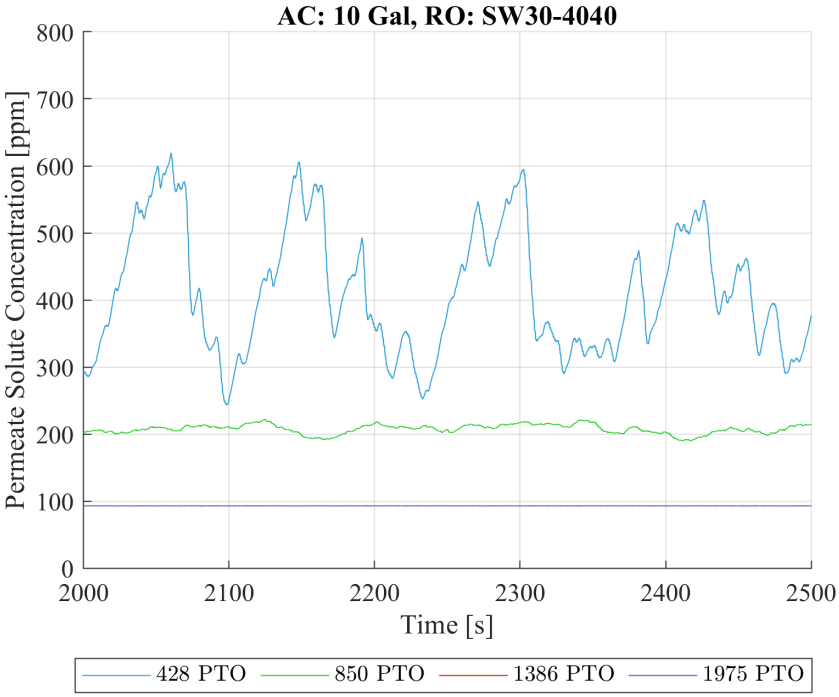

Figure 4.9: The Effect of the PTO Volumetric Displacement on The Permeate Solute Concentration.

As seen in Figure 4.7, the 428 cm^3/rad PTO displacement was not able to reach the minimum feed flow rate required by the SW30-4040 RO membrane. Additionally, Figure 4.9 shows that the permeate solute concentration reached above 500 ppm for the system using a 428 cm^3/rad PTO displacement with the SW30-4040 RO membrane, which is above 500 ppm standard for drinking water set by the U.S. EPA[34]. The 850 cm^3/rad PTO displacement was only slightly above the minimum feed flow rate required by the SW30-4040 RO membrane. However, the next largest PTO displacement, 1386 cm^3/rad, operated at the maximum feed pressure, which is shown in Figure 4.8. This could indicate that the ideal PTO volumetric displacement for a single SW30-4040 RO membrane is somewhere between 850 cm^3/rad and 1386 cm^3/rad. Likewise, for the SW-2540 RO membrane, the 850 cm^3/rad PTO displacement operated at the maximum feed pressure, whereas the 428 cm^3/rad PTO displacement operated at an average feed flow rate of 1.892 gpm compared to the minimum

required feed flow rate of 1.23 gpm for the SW30-2540 RO membrane. This could indicate that the ideal PTO volumetric displacement for the SW30-2540 RO membrane is somewhere between 428 cm^3/rad and 850 cm^3/rad.

4.4 Optimal Case Analysis

The three cases with the highest water production rates were the SW30HR-380 RO membrane with the 1975 cm^3/rad PTO displacement and a 10-gallon accumulator volume, the SW30-4040 RO membrane with the 1386 cm^3/rad PTO displacement and a 10-gallon accumulator volume, and the SW30-4040 RO membrane with the 850 cm^3/rad PTO displacement and a 10-gallon accumulator volume. The case that resulted in the highest water production rate by the system was the case that used the SW30HR-380 RO membrane, a 10-gallon accumulator, and a PTO volumetric displacement of 1975 cm^3/rad. Figure 4.10 shows a plot of the water production rate for this case. This combination of parameters resulted in an average water production rate of 32.644 gpm, with 4.081 gpm produced by the RO system and 28.563 gpm produced by the SCWD system. The average feed pressure into the RO system was 41.991 bar. Figure 4.11 shows a plot of the RO feed pressure. For the case with the highest water production rate, the average permeate solute concentration was 104.79 ppm, which is in the desired range of less than 300 ppm. Figure 4.12 shows a plot of the permeate solute concentration.

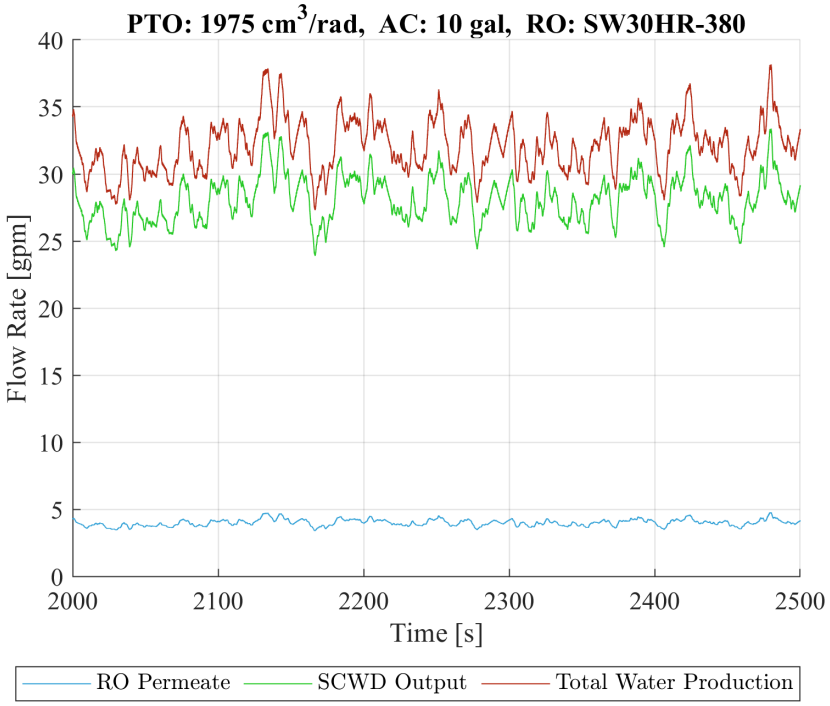

Figure 4.10: Water Production Rate for a System Using an SW30HR-380 RO Membrane, 1975 cm^3/rad PTO Volumetric Displacement, and a 10-Gallon Accumulator.

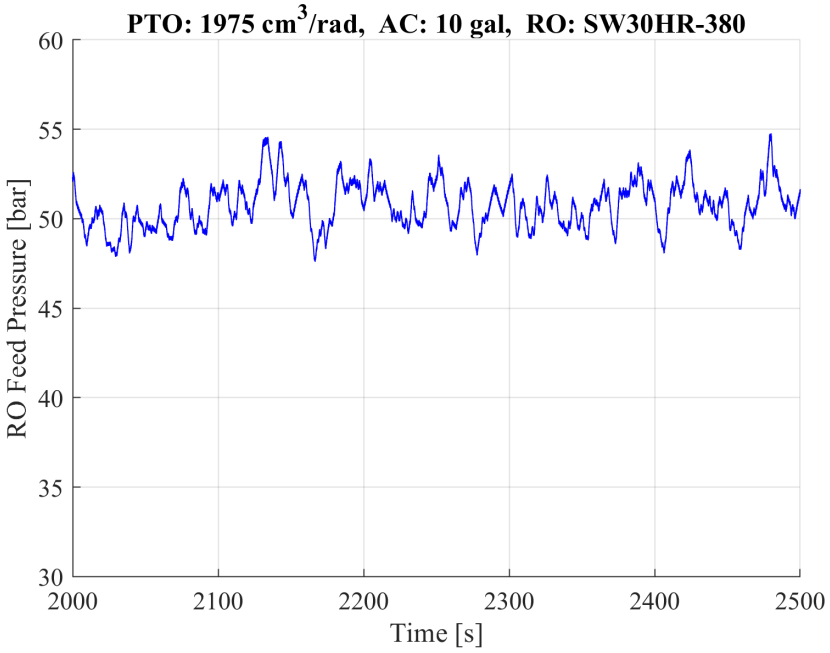

Figure 4.11: RO Feed Pressure for a System Using an SW30HR-380 RO Membrane, 1975 cm^3/rad PTO Volumetric Displacement, and a 10-Gallon Accumulator.

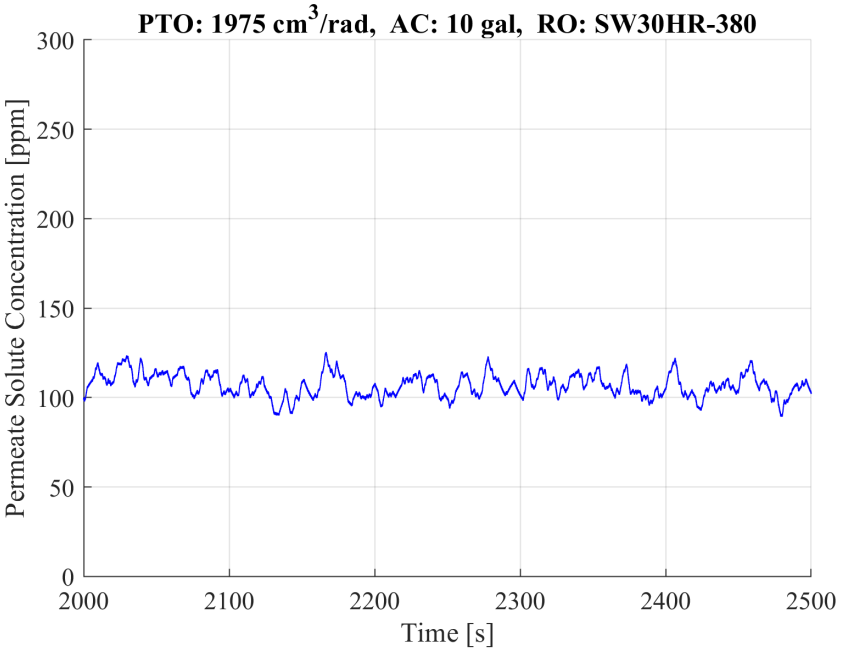

Figure 4.12: Permeate Solute Concentration for a System Using an SW30HR-380 RO Membrane, 1975 cm^3/rad PTO Volumetric Displacement, and a 10-Gallon Accumulator.

The case that resulted in the second highest water production rate was the case that used the SW30-4040 RO membrane, a 10-gallon accumulator, and a PTO volumetric displacement of 1386 cm^3/rad. This combination of parameters resulted in an average water production rate of 11.367 gpm, with 1.421 gpm produced by the RO system and 9.946 gpm produced by the SCWD system. However, the system reached the maximum feed pressure going into the RO membrane, which was 57 bar. As a result, a substantial amount of pressurized seawater was lost through the pressure relief valve, which is why the flow rates out of the RO and SCWD systems are constant. Additional membranes could potentially be added to increase the recovery ratio of the RO system since this PTO was able to operate above the limits for a system with a single RO membrane. Figure 4.13 shows a plot of the water production rate for this case, and Figure 4.14 shows a plot of the RO feed pressure. The average permeate solute concentration was 93.125 ppm, which is in the desired range of less than 300 ppm. Figure 4.15 shows a plot of the permeate solute concentration.

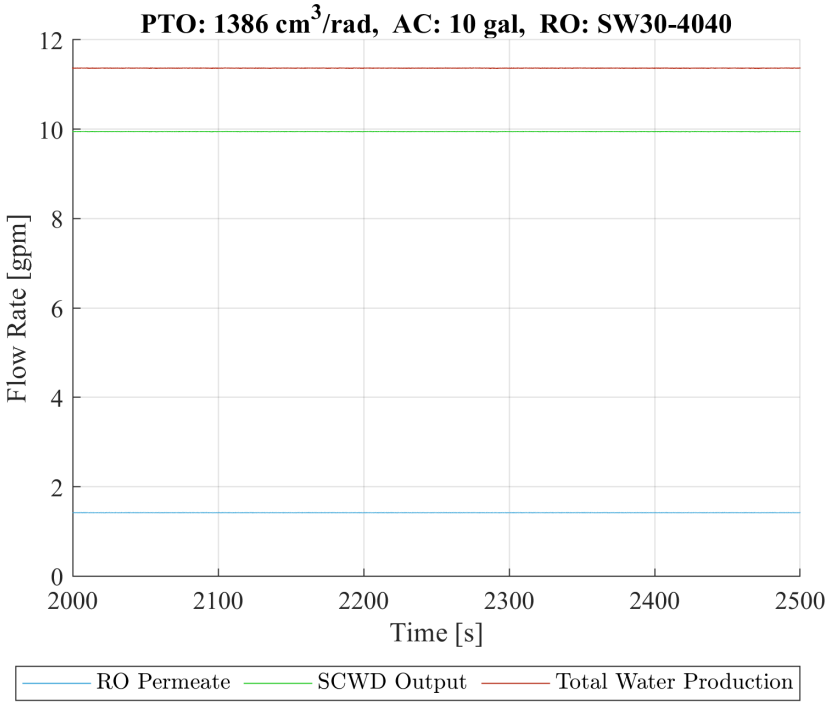

Figure 4.13: Water Production Rate for a System Using an SW30-4040 RO Membrane, 1386 cm^3/rad PTO Volumetric Displacement, and a 10-Gallon Accumulator.

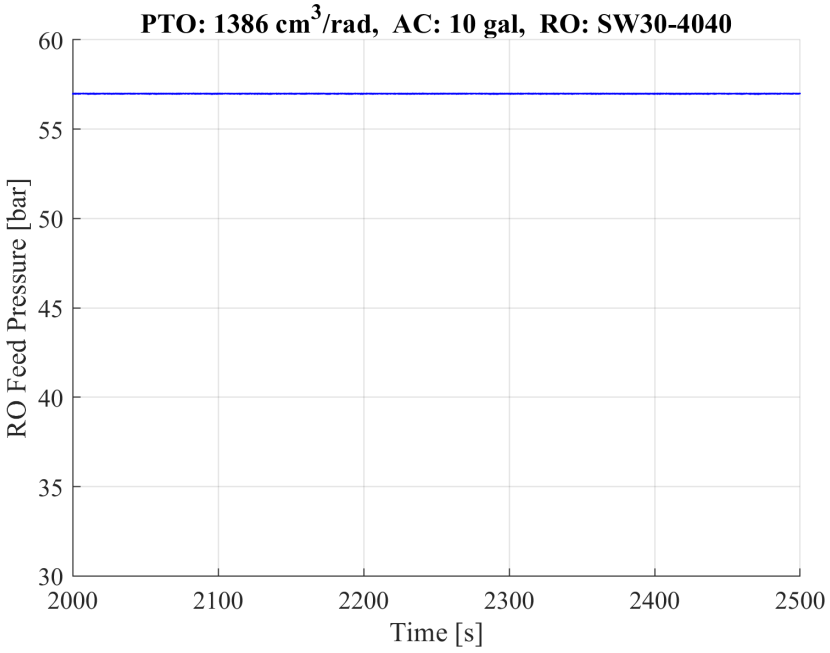

Figure 4.14: RO Feed Pressure for a System Using an SW30-4040 RO Membrane, 1386 cm^3/rad PTO Volumetric Displacement, and a 10-Gallon Accumulator.

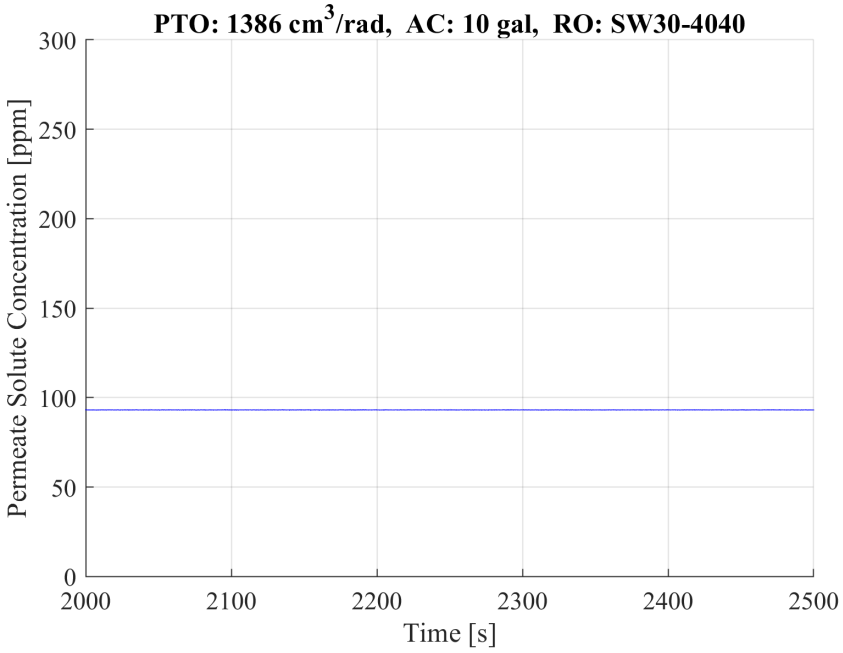

Figure 4.15: Permeate Solute Concentration for a System Using an SW30-4040 RO Membrane, 1386 cm^3/rad PTO Volumetric Displacement, and a 10-Gallon Accumulator.

The case that resulted in the third highest water production rate was the case that used the SW30-4040 RO membrane, a 10-gallon accumulator, and a PTO volumetric displacement of 850 cm^3/rad. This combination of parameters resulted in an average water production rate of 5.084 gpm, with 0.635 gpm produced by the RO system and 4.448 gpm produced by the SCWD system. Figure 4.16 shows a plot of the water production rate for this case. This case had a relatively low amount of hydraulic fluctuations entering the RO membrane and operated in the desired pressure range. The average RO feed pressure was 41.991 bar. Figure 4.17 shows a plot of the RO feed pressure. Additionally, it had an average permeate solute concentration of 209.195 ppm, which is in the desired range of less than 300 ppm. Figure 4.18 shows a plot of the permeate solute concentration.

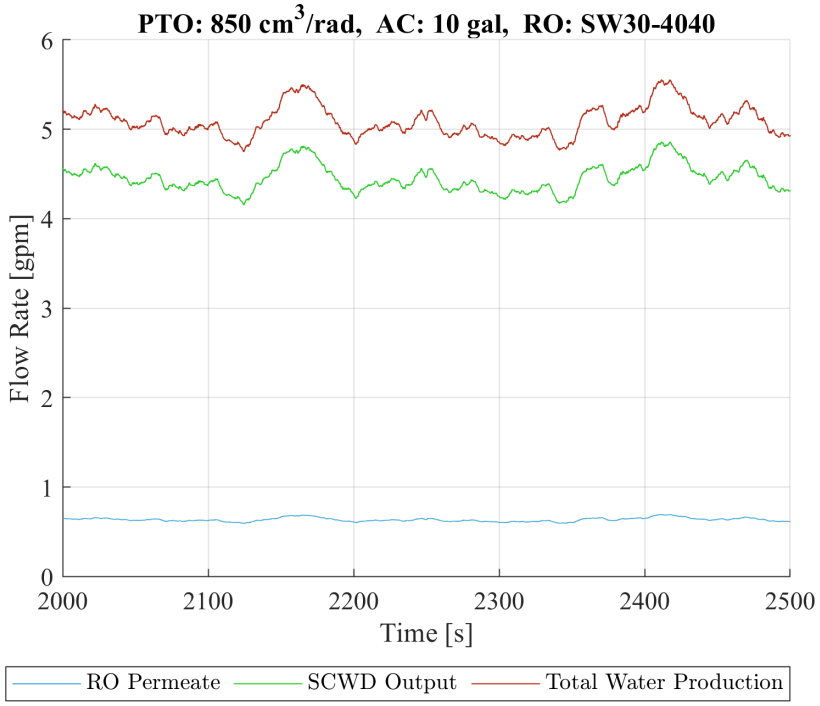

Figure 4.16: Water Production Rate for a System Using an SW30-4040 RO Membrane, 850 cm^3/rad PTO Volumetric Displacement, and a 10-Gallon Accumulator.

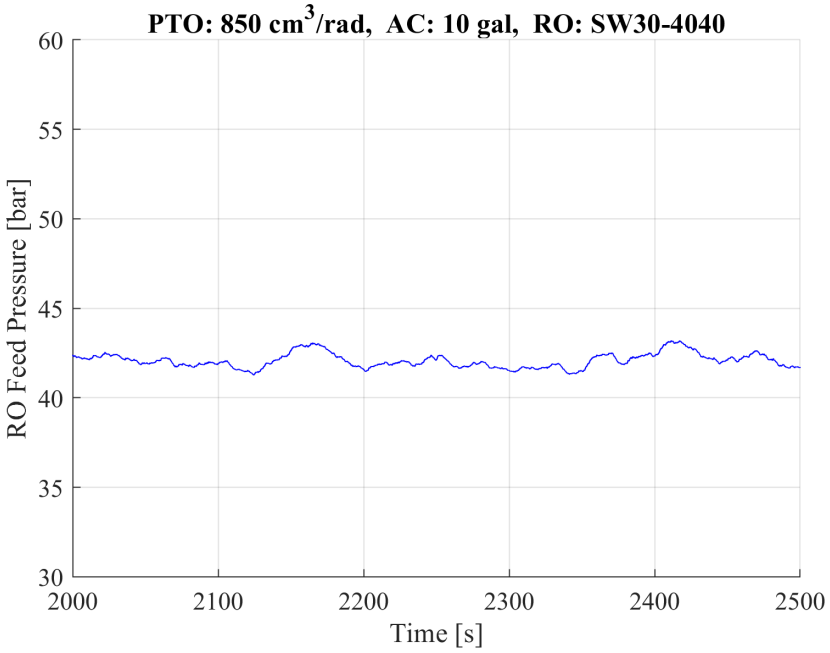

Figure 4.17: RO Feed Pressure for a System Using an SW30-4040 RO Membrane, 850 cm^3/rad PTO Volumetric Displacement, and a 10-Gallon Accumulator.

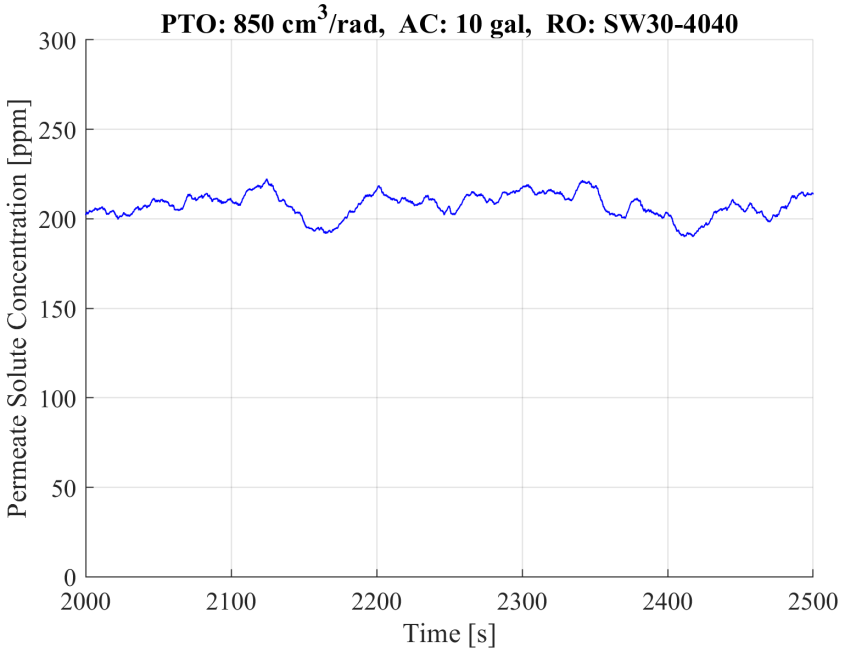

Figure 4.18: Permeate Solute Concentration for a System Using an SW30-4040 RO Membrane, 850 cm^3/rad PTO Volumetric Displacement, and a 10-Gallon Accumulator.

From the 72 cases tested in the sensitivity analysis, the optimal case was determined to be the one using the SW30HR-380 RO membrane, the 1975 cm^3/rad PTO volumetric displacement, and the 10-gallon accumulator. This case had the highest water production rate, and the quality of the produced water was in the desired range. A summary of the average water production rates and the permeate solute concentrations for the top 3 cases is contained in Table 4.1.

Table 4.1: Result Summary for the Top Three Cases (with a 10-Gallon Accumulator)

RO Membrane	PTO Displacement [cm^3/rad]	Average Total Water Production Rate [gpm]	Average RO Permeate Flow Rate [gpm]	Average SCWD Water Production Rate [gpm]	Average Permeate Solute Concentration [ppm]
SW30HR-380	1975	32.644	4.081	28.563	104.790
SW30-4040	1386	11.367	1.421	9.946	93.125
SW30-4040	850	5.084	0.635	4.448	209.195

Chapter 5

Conclusion

The developed numerical model of the zero-waste wave-to-water desalination system was described in Section 3. The results of the sensitivity analysis were presented in Section 4. The sensitivity analysis showed the accumulator volume had a minimal effect on the total amount of water produced but instead had a significant effect on the amount of hydraulic fluctuations entering the RO system. The type of RO membrane and the PTO volumetric displacement both had a significant impact on the amount of water produced by the system. The optimal system configuration was the SW30HR-380 RO membrane, 1975 cm^3/rad PTO volumetric displacement, and a 10-gallon accumulator. The optimized system had an average total water production rate of 32.644 gpm, with 4.081 gpm from the RO system and 28.563 gpm from the SCWD system. The average permeate solute concentration was 104.790 ppm. The results of this research demonstrated the potential of the zero-waste wave-to-water desalination system to address the increasing water demand while reducing the environmental impact caused by brine disposal.

Chapter 6

Recommendations for Future Work

There are several recommendations for future work to add to the findings of this research. The first recommendation is to expand the sensitivity analysis to include more parameters, such as the number of RO membranes and the wave conditions. Incorporating more RO membranes would allow the system to operate at a higher recovery ratio, which could lead to a reduced cost. Including the wave conditions in the sensitivity analysis could help determine which parameters can operate under the widest range of wave conditions commonly found in the intended application area.

Additionally, the current eight PTO volumetric displacements and three RO membrane types tested in this sensitivity analysis could be expanded to include more values. Testing more values in the sensitivity analysis would allow for a more comprehensive understanding of the system's performance across a wider range of parameters. The sensitivity analysis results presented in this thesis indicated that the largest PTO volumetric displacement led to the largest water production rate. However, there is a limit to the PTO size that could work for the 1:15 scale system. Expanding the sensitivity analysis to test more values could help determine the maximum and minimum PTO volumetric displacements that could work for each membrane type.

The second recommendation is to perform an economic analysis that considers the cost of each parameter. While larger PTO displacements and RO membrane types produced more water, they are also more expensive than the smaller sizes. An economic analysis that considers the costs of the parameters could help identify the combination of parameters that produces water at the lowest cost, which could be used to optimize the system's cost-effectiveness.

The third recommendation is to develop a small-scale prototype of the entire system to validate the complete numerical model. This would allow for real-world testing and validation of the model's predictions, which could potentially lead to improvements and refinements of the model for future use.

The final recommendation is to incorporate either a solar energy system or a two-WEC system to provide the power the SCWD system needs. Adding either of these to the model could provide additional power to the system, which could help identify the optimal system configuration. A solar energy system could help provide thermal energy to heat the fluid in the SCWD system. A two-WEC system could help with increasing the pressure of the fluid for the SCWD system. Adding either of these to the model would help identify the optimal system configuration based on the additional power these components could provide compared to the energy required by the SCWD system.

References

[1] M. M. Mekonnen and A. Y. Hoekstra, "Four billion people facing severe water scarcity," vol. 2, no. 2, p. e1500323, publisher: American Association for the Advancement of Science. [Online]. Available: https://www.science.org/doi/10.1126/sciadv.1500323

[2] R. I. McDonald, K. Weber, J. Padowski, M. Flörke, C. Schneider, P. A. Green, T. Gleeson, S. Eckman, B. Lehner, D. Balk, T. Boucher, G. Grill, and M. Montgomery, "Water on an urban planet: Urbanization and the reach of urban water infrastructure," vol. 27, pp. 96–105. [Online]. Available: https://www.sciencedirect.com/science/article/pii/S0959378014000880

[3] K. Mullen. Information on earth's water. [Online]. Available: https://www.ngwa.org/what-is-groundwater/About-groundwater/information-on-earths-water

[4] E. Jones, M. Qadir, M. T. H. van Vliet, V. Smakhtin, and S.-m. Kang, "The state of desalination and brine production: A global outlook," *Science of The Total Environment*, vol. 657, pp. 1343–1356, Mar. 2019. [Online]. Available: https://www.sciencedirect.com/science/article/pii/S0048969718349167

[5] J. Morillo, J. Usero, D. Rosado, H. El Bakouri, A. Riaza, and F.-J. Bernaola, "Comparative study of brine management technologies for desalination plants," *Desalination*, vol. 336, pp. 32–49, Mar. 2014. [Online]. Available: https://www.sciencedirect.com/science/article/pii/S0011916414000071

[6] A. LiVecchi, A. Copping, D. Jenne, A. Gorton, R. Preus, G. Gill, R. Robichaud, R. Green, S. Geerlofs, S. Gore, D. Hume, W. McShane, C. Schmaus, and H. Spence, "Exploring opportunities for marine renewable energy in maritime markets," pp. 86–98.

[7] M. Wales. The cost of renewable energy versus fossil fuels. [Online]. Available: https://www.naturespath.com/en-us/blog/cost-renewable-energy-versus-fossil-fuels/

[8] Prasanna. Advantages and disadvantages of wave energy | various top advantages and disadvantages of wave energy. [Online]. Available: https://www.aplustopper.com/advantages-and-disadvantages-of-wave-energy/

[9] WEC-sim (wave energy converter SIMulator) — WEC-sim documentation. [Online]. Available: https://wec-sim.github.io/WEC-Sim/master/index.html

[10] E. J. Okampo and N. Nwulu, "Optimisation of renewable energy powered reverse osmosis desalination systems: A state-of-the-art review," vol. 140, p. 110712. [Online]. Available: https://www.sciencedirect.com/science/article/pii/S1364032121000095

[11] J. Tonner, "Barriers to thermal desalination in the united states."

[12] A. Al-Karaghouli and L. L. Kazmerski, "Energy consumption and water production cost of conventional and renewable-energy-powered desalination processes," *Renewable and Sustainable Energy Reviews*, vol. 24, pp. 343–356, Aug. 2013. [Online]. Available: https://www.sciencedirect.com/science/article/pii/S1364032113000208

[13] S. Sethi and G. Wetterau, "Seawater desalination overview," p. 13.

[14] S. van Wyk, S. O. Odu, A. G. J. van der Ham, and S. R. A. Kersten, "Design and results of a first generation pilot plant for supercritical water desalination (SCWD)," *Desalination*, vol. 439, pp. 80–92, Aug. 2018. [Online]. Available: https://www.sciencedirect.com/science/article/pii/S0011916417325365

[15] S. O. Odu, A. G. J. van der Ham, S. Metz, and S. R. A. Kersten, "Design of a process for supercritical water desalination with zero liquid discharge," vol. 54, no. 20, pp. 5527–5535, publisher: American Chemical Society. [Online]. Available: https://doi.org/10.1021/acs.iecr.5b00826

[16] N. A. Moharram, S. Bayoumi, A. A. Hanafy, and W. M. El-Maghlany, "Hybrid desalination and power generation plant utilizing multi-stage flash and reverse osmosis driven by parabolic trough collectors," vol. 23, p. 100807. [Online]. Available: https://www.sciencedirect.com/science/article/pii/S2214157X20305499

[17] A. Panagopoulos, K.-J. Haralambous, and M. Loizidou, "Desalination brine disposal methods and treatment technologies - A review," *Science of The Total Environment*, vol. 693, p. 133545, Nov. 2019. [Online]. Available: https://www.sciencedirect.com/science/article/pii/S0048969719334655

[18] P. Xu, T. Y. Cath, A. P. Robertson, M. Reinhard, J. O. Leckie, and J. E. Drewes, "Critical Review of Desalination Concentrate Management, Treatment and Beneficial Use," *Environmental Engineering Science*, vol. 30, no. 8, pp. 502–514, Aug. 2013, publisher: Mary Ann Liebert, Inc., publishers. [Online]. Available: https://www.liebertpub.com/doi/10.1089/ees.2012.0348

[19] R. Katal, T. Y. Shen, I. Jafari, S. Masudy-Panah, M. H. D. A. Farahani, R. Katal, T. Y. Shen, I. Jafari, S. Masudy-Panah, and M. H. D. A. Farahani, *An Overview on the Treatment and Management of the Desalination Brine Solution*. IntechOpen, Jun. 2020, publication Title: Desalination - Challenges and Opportunities. [Online]. Available: https://www.intechopen.com/chapters/72467

[20] E. Amini, R. Asadi, D. Golbaz, M. Nasiri, S. T. O. Naeeni, M. Majidi Nezhad, G. Piras, and M. Neshat, "Comparative study of oscillating surge wave energy converter performance: A case study for southern coasts of the caspian sea," vol. 13, no. 19, p. 10932, number: 19 Publisher: Multidisciplinary Digital Publishing Institute. [Online]. Available: https://www.mdpi.com/2071-1050/13/19/10932

[21] E. Amini, H. Mehdipour, E. Faraggiana, D. Golbaz, S. Mozaffari, G. Bracco, and M. Neshat, "Optimization study of hydraulic power take-off system for an ocean wave energy converter." [Online]. Available: http://arxiv.org/abs/2112.09803

[22] Y.-H. Yu and D. Jenne, "Analysis of a wave-powered, reverse-osmosis system and its economic availability in the united states," vol. 10, p. V010T09A032. [Online]. Available: https://asmedigitalcollection.asme.org/OMAE/proceedings/OMAE2017/57786/Trondheim,%20Norway/282142

[23] Y.-H. Yu and D. Jenne, "Numerical modeling and dynamic analysis of a wave-powered reverse-osmosis system," vol. 6, no. 4, p. 132, number: 4 Publisher: Multidisciplinary Digital Publishing Institute. [Online]. Available: https://www.mdpi.com/2077-1312/6/4/132

[24] F. Filho, G. Glosson, J. McMorris, T. Abdel-Salam, K. Duba, T. T. Tran, and S. Husain, "A Novel Zero-Discharge Supercritical Water-Based Wave Energy Desalination System." American Society of Mechanical Engineers Digital Collection, Oct. 2022. [Online]. Available: https://asmedigitalcollection-asme-org.eu1.proxy.openathens.net/OMAE/proceedings-abstract/OMAE2022/85932/1148056

[25] "Wamit, Inc. - The State of the Art in Wave Interaction Analysis." [Online]. Available: https://www.wamit.com/techdescription.htm

[26] Advanced features — WEC-sim documentation. [Online]. Available: https://wec-sim.github.io/WEC-Sim/master/user/advanced_features.html#user-advanced-features-bemio

[27] Overview — WEC-sim documentation. [Online]. Available: https://wec-sim.github.io/WEC-Sim/master/theory/theory.html

[28] J. G. Wijmans and R. W. Baker, "The solution-diffusion model: a review," *Journal of Membrane Science*, vol. 107, no. 1, pp. 1–21, Nov. 1995. [Online]. Available: https://www.sciencedirect.com/science/article/pii/037673889500102I

[29] E. Nagy, "Chapter 21 - Pressure-Retarded Osmosis (PRO) Process," in *Basic Equations of Mass Transport Through a Membrane Layer (Second Edition)*, E. Nagy, Ed. Elsevier, Jan. 2019, pp. 505–531. [Online]. Available: https://www.sciencedirect.com/science/article/pii/B9780128137222000212

[30] "WAVE Water Treatment Design Software." [Online]. Available: https://www.dupont.com/water/resources/design-software.html

[31] M. Rahman, M. M. Sohel, and F. Ahmed, "Physico-chemical and bacteriological analysis of drinking tube-well water from some primary school, Magura, Bangladesh to evaluate suitability for students," *Int. Journal of Applied Sciences and Engineering Research*, vol. 4, Oct. 2015.

[32] M. R. Islam, M. K. I. Sarkar, T. Afrin, S. S. Rahman, R. I. Talukder, B. K. Howlader, and M. A. Khaleque, "A Study on Total Dissolved Solids and Hardness Level of Drinking Mineral Water in Bangladesh," *American Journal of Applied Chemistry*, vol. 4, no. 5, p. 164, Aug. 2016, number: 5 Publisher: Science Publishing Group. [Online]. Available: https://www.sciencepublishinggroup.com/journal/paperinfo?journalid=227&paperId=10015955

[33] O. Ojo, "Ojo, O. O. S. and Awokola, O. S., 2012. "Determination of Groundwater Physiochemical Parameters of shallow Aquifers in Agbowo and Ajibode communities in Oyo State, South Western Nigeria". International Journal of Engineering Research and Development e-ISSN: 2278-067X, p-ISSN: 2278-800X Volume 3, Issue 5 (August 2012), PP. 10-23," *International Journal of Engineering Research and Development*, vol. Volume 3, pp. PP. 10–23, Aug. 2012.

[34] E. R. Merriam, M. P. Strager, and J. T. Petty, "Source water vulnerability to elevated total dissolved solids within a mixed-use Appalachian River basin," *PLOS Water*, vol. 1, no. 8, p. e0000035, Aug. 2022, publisher: Public Library of Science. [Online]. Available: https://journals.plos.org/water/article?id=10.1371/journal.pwat.0000035

[35] S. Wimalawansa, "Purification of Contaminated Water with Reverse Osmosis: Effective Solution of Providing Clean Water for Human Needs in Developing Countries," *Int. J. Emerging Technology Adv. Engin*, vol. 9001, Dec. 2013.

[36] "MATLAB Variable Area Hydraulic Orifice." [Online]. Available: https://www.mathworks.com/help/simscape/ref/variableareahydraulicorifice.html

[37] J. Chen, Personal Communication, East Carolina University, June 2022.